N5 is the New C4a: Biochemical Functionalization of Reduced Flavins at the N5 Position

Brett A. Beaupre and Graham R. Moran†

Department of Chemistry and Biochemistry, 1068 W Sheridan Rd, Loyola University Chicago, Chicago, IL 60660.

†Corresponding author; phone: (773)508-3756; email: gmoran3@luc.edu

This research was supported by National Science Foundation Grant 1904480 to G.R.M.

Introduction

Flavins are requisite to all life and are utilized as cofactors by enzymes throughout primary and secondary metabolism. They are typically enlisted by enzymes to facilitate oxidation/reduction reactions where the isoalloxazine ring system acts as a redox mediator or conduit between two other chemicals. Flavins are uniquely versatile in such reactions as the isoalloxazine can stabilize four reduction states: four-electron oxidized, two-electron oxidized, one-electron oxidized and reduced. In addition to redox chemistries, flavins have been shown to facilitate reactions where no net redox change occurs[1]. In such reactions, the reduced isoalloxazine ring acts as a nucleophile to generate covalent intermediates. Flavins extend their biochemical utility by covalent modification of the isoalloxazine either as an indelible modification or as a transient adduct (Figure 1). While covalent modifications of the C4a position have been known and studied for five decades, recently the versatility of the N5 position has come to the fore. Multiple lineages of flavin enzymes are now known to have evolved the capacity to form unique covalent modifications at the flavin N5 position that expand the known repertoire of flavin catalyzed reactions.

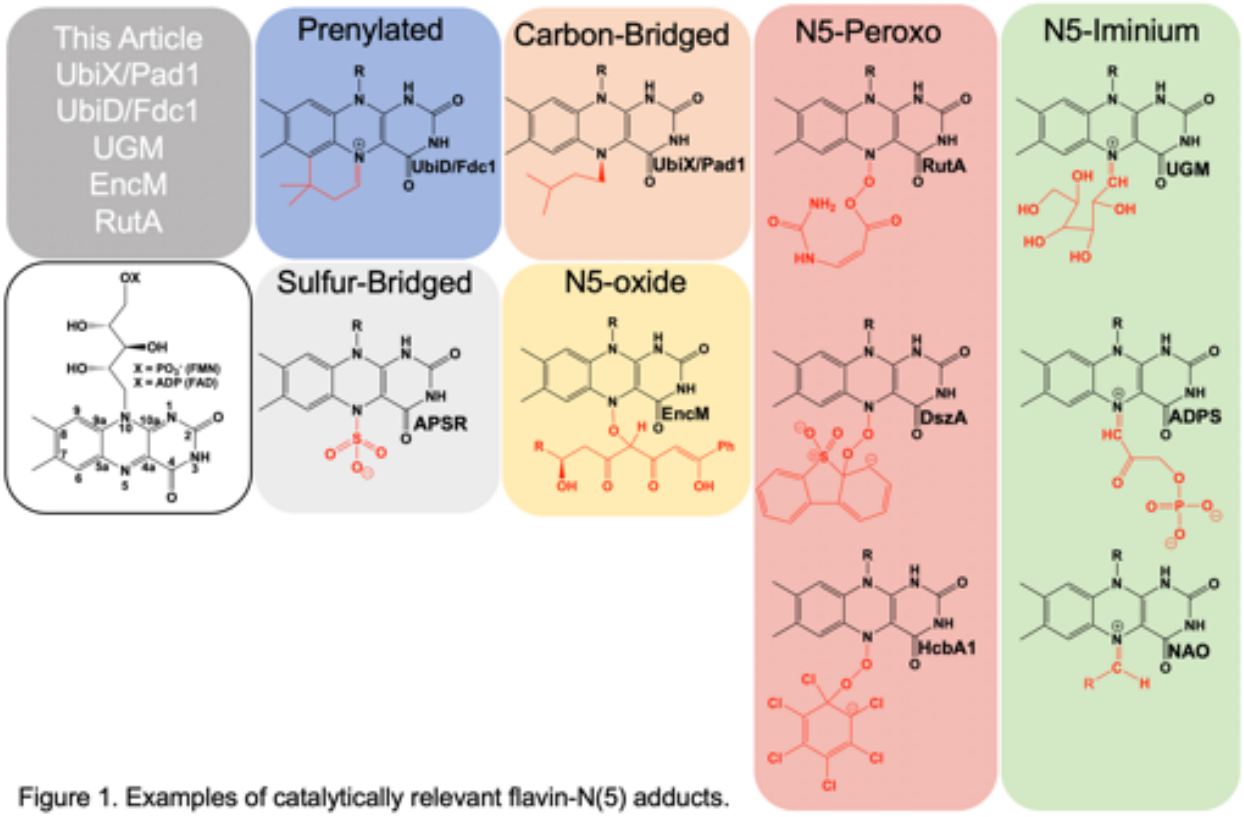

Figure 1. Examples of catalytically relevant flavin-N(5) adducts.

Formally, the most common functionalization of the flavin N5 position occurs with hydride transfer from a reductant substrate to form an N5-H adduct (reduced flavin). However, the ubiquity of this species in flavoprotein oxidases, dehydrogenases and other flavoenzymes precludes description in this article. Functionalization of an N5 by a moiety other than hydrogen was first described in 1967 when a photoalkylated C4a-lumiflavin adduct underwent isomerization[2]. Soon after numerous examples of native and non-native N5 sulfite adducts with. the oxidized isoalloxazine were described[3-7]. N5 adducts formed in non-native reactions with flavo-enzymes are reported from 1970 onward[6, 8-14]. However, it wasn't until 1997 that the first verified example of a catalytically relevant N5 adduct forming with the reduced flavin of nitroalkane oxidase (NAO) was reported by Gadda et al[15]. Soon after a native sulfate adduct was

shown crystallographically in adenylylsulfate reductase(APSR)[16]. These discoveries solidified the notion of two primary adjacent catalytic centers in reduced flavin cofactors, C4a and N5.

In this article, we present recently identified flavo-enzymes that incorporate N5 modifications either during catalysis (intermediates) or as cofactor modification/maturation processes. This includes a pair isofunctional enzymes that form an N5-carbon adduct to catalyze the generation of a prenylated flavin mononucleotide (UbiX/Pad1) that is then utilized as a cofactor by prenylated flavin-dependent non-oxidative decarboxylase enzymes (UbiD/Fdc1). It also describes an example of a redox-neutral flavin reaction that uses the two-electron reduced flavin in catalysis and transiently forms an N5-galactose linkage (UGM). Lastly N5 oxo forms are presented; these utilize either the hyper-oxidized flavin N5-oxide (EncM) or the flavin N5-peroxide (RutA) to carry out oxygenation reactions.

Prenylated: UbiX UbiD, Pad1 and Fdc1

The bacterial genes *ubiX* and *ubiD* and their respective fungal homologs *pad1* and *fdc1* encode for two pairs of enzymes associated with a reversible, non-oxidative decarboxylation of an aromatic substrate[17-20]. These are essential steps in the biosynthesis of prokaryotic ubiquinone [17, 18, 21-23] or fungal degradation of phenylacrylic/aromatic acids[24-27]. Due to similarities in the phenotype of gene deletion mutants, the proteins UbiX and UbiD, Pad1 and Fdc1 were initially believed to be isofunctional (despite minimal sequence similarity). Both sets of proteins where expressed together and thought to have redundant catalytic activity where bacterial UbiX and UbiD catalyze the decarboxylation of 3-octaprenyl-4-hydroxybenzoate to 2-octaprenylphenol[22, 26, 28-31] and eukaryotic Pad1 and Fdc1 catalyze the decarboxylation of cinnamic acid, coumaric

acid and ferulic acid to styrene, 4-vinyl phenol and 4-vinyl benzene [24, 26, 27, 32]. In 2015 it was determined that UbiX was in fact isofunctional with Pad1 and that neither possesses decarboxylase activity[33]. Instead both function as prenyltransferases, catalyzing the formation of a prenylated four-ring flavin mononucleotide that is the cofactor for non-oxidative reversible decarboxylation reactions catalyzed by the UbiD and Fdc1 enzymes[34, 35] (Scheme 1).

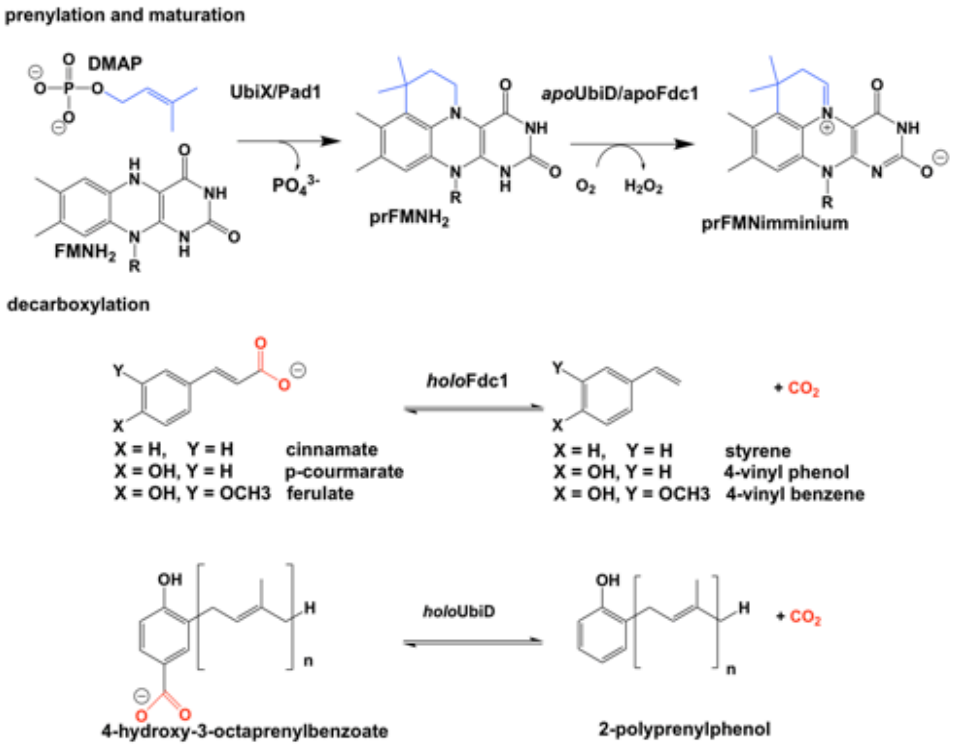

Scheme 1. Overview of the proposed reaction of UbiX, UbiD, Pad1 and Fdc1.

Reduced flavin mononucleotide ($FMNH_2$) is prenylated by UbiX and Pad1. The N5-C6-prenylated flavin mononucleotide ($prFMNH_2$) is bound as an immature cofactor by apoUbiD/apoFdc1 and then oxidized to the catalytically active prenylated flavin mononucleotide iminium ion ($prFMN_{iminium}$) form (Scheme 1). While decarboxylation reactions are not uncommon in the chemistries of living organisms and there are multiple examples of the enzymatic use of

unmodified flavin for decarboxylation[36-38], the use of a prenylated FMN[34] for this chemistry was unprecedented.

The first structural insights into UbiX/Pad1 came with a 1.5 Å resolution crystal structure of UbiX from *Psuedomonas aeruginosa*[39] (PDB CODE 3ZQU). It was observed that UbiX assembles into a dodecamer and binds FMN using Rossman fold motif at the interface between three subunits. Crystal structures also revealed a small hydrophilic pocket adjacent to the *re*-face of the isoalloxazine moiety constructed of residues from the three proximal subunits and that neither face of the isoalloxazine was accessible to bulk solvent. Structural similarities to multiple enzymes related to decarboxylase activity[37, 38, 40-42] was one of the factors that initially prompted UbiX and Pad1 to be classified as FMN-dependent decarboxylase enzymes. However, no activity was seen when UbiX was incubated with substrate analogs 4-hydroxybenzoic acid, vanillic acid and 3-carboxymethyl amino-methyl-4-hydroxybenzoic acid and a classic redox role for FMN in the decarboxylation of benzoic acid derivatives (the apparent substrates of UbiD/UbiX) could not be established[39].

In 20010 Mukai et al. examined a prior study (Ago, S., Kawasaki, H., and Kikuchi Y., Abst. 50th Annu. Meet. Soc. Biothechnol. p.24, 1998) that demonstrated saké yeast, normally devoid of ferulic acid decarboxylase activity due to lack of the *fdc1* gene, could exhibit resistance to ferulic acid when the gene *fdc1* (YDR539W) from wine yeast was incorporated into its genome indicating that Pad1/Fdc1 (UbiX/UbiD) are not isofunctional and that expression of both genes is required for decarboxylation activity. Confirmation came when it was demonstrated that cessation of decarboxylase activity in *Saccharomyces cerevisea* occurred with the deletion of

either the *fdc1* or *pad1* gene and that the resulting phenotype of either mutant was identical to the double mutant[25].

Researchers from the University of Michigan proposed Pad1 and Fdc1 are part of a two component decarboxylase system where Pad1 activates Fdc1 and suggested it does so by providing Fdc1 with a covalently modified flavin mononucleotide cofactor[33]. On this basis UbiX was incubated with oxidized FMN and dimethylallyl monophosphate (DMAP) and perturbation of the FMN UV-visible spectrum was observed[34], suggesting that DMAP binds in close proximity to the oxidized flavin. The binding of dimethylallyl monophosphate (DMAP) was confirmed by solving the crystal structure of the UbiX•FMN_{ox}•DMAP complex (PDB CODE 4ZAF, 1.7 Å) [34] where DMAP binds adjacent to the *re*-face of the isoalloxazine moiety of the flavin monophosphate in a hydrophobic pocket reminiscent of that observed in terpene synthases and prenyl transferases[43-45] (Figure 2A).

The identity of the modified flavin mononucleotide produced by UbiX and Pad1 was determined when UbiX from *Pseudomonas aeruginosa* was incubated with reduced flavin mononucleotide ($FMNH_2$) and DMAP resulting in the formation of a prenylated flavin mononucleotide ($prFMNH_2$)[34] (Figure 2B). Crystals of UbiX could undergo turnover allowing researchers to use time-dependent crystallography matched with mass spectroscopy and/or UV visible spectroscopy to (1) confirm the binding of DMAP to the oxidized UbiX FMN (UbiX•FMN_{ox}•DMAP)(PDB CODE 4ZAF), (2) show the structure of the active UbiX•$FMNH_2$ complex (Glu49Gln variant UbiX•$FMNH_2$•DMAP complex)(PDB CODE 4ZAL, 1.6 Å), (3) capture the initial N5-C1' alkyl adduct (PDB CODE 4ZAV, 1.4 Å), (4) the product complex (UbiX•$prFMNH_2$) (PDB CODE 4ZAW, 1.9 Å) and (5) observe the oxidation of the $prFMNH_2$ to the purple oxygen

dependent radical species (UbiX•prFMN$_{radical}$)(PDB CODE 4ZAX, 1.6 Å) (Figure 2). Each of these structures formed sequentially when UbiX-FMN$_{ox}$-DMAP was incubated with sodium dithionite [34].

The structures in support of the proposed chemical mechanism in this sequence are shown in Figure 2 with a summary of the mechanism proposed from these structures. Active site mutations of UbiX revealed large conformational changes occur after reduction to yield species B that was then transformed to the stable N5 adduct C, before forming of the product, D [34].

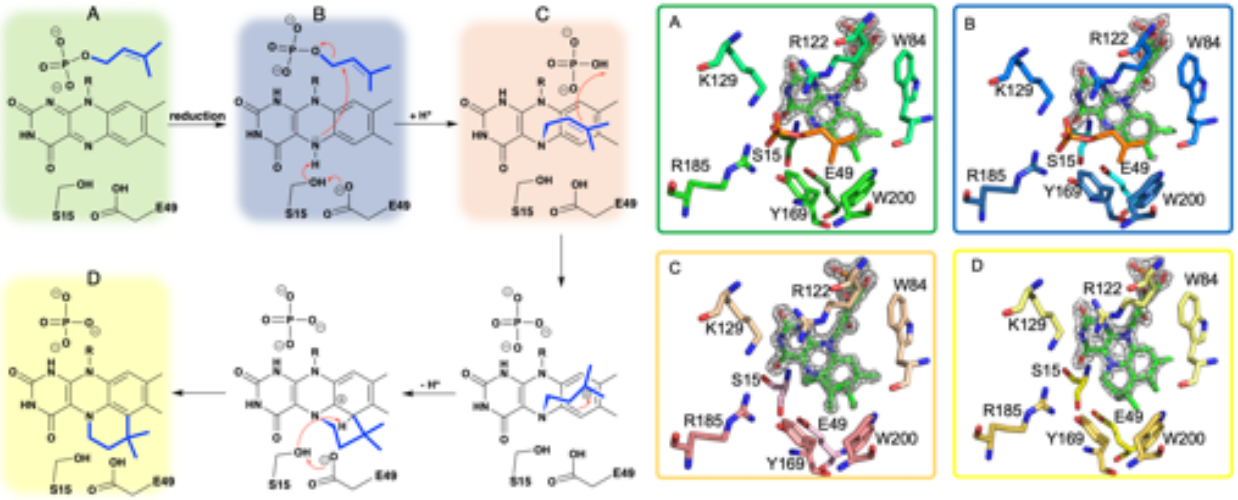

Figure 2. A hypothetical chemical mechanism for UbiX/Pad1 and supporting crystal structures of A. UbiX$_{ox}$•DMP (dimethylallyl monophosphate) complex (PDB code 4ZAF), B. UbiX$_{red}$•IMP (isopentyl monophosphate) complex (PDB code 6QLH), C. UbiX-dimethylallyl monophosphate adduct (PDB code 4ZAV), D. UbiX•FMN$_{pren}$ complex (PDB code 4ZAW).

Ubix/Pad1 offers the first example of a flavin monophosphate dependent prenyl-transferase and forms a new flavin cofactor, an bridged N5 and C6 dimethyl prenylflavin. The enzymes UbiX and Fdc1 ensure a stable N5-alkyl adduct flavin species (prFMNH$_2$) is favored over the reactive N5-iminium adduct (prFMN$_{iminium}$) by utilizing the reduced from of the flavin monophosphate to act as a nucleophile. This strategy dictates that the reduced prenylated flavin monophosphate product of UbiX/Pad1 is transferred to apo-UbiD/Fdc1 before undergoing activation/oxidation to the reactive imine form.

When the *fdc1* gene from *Aspergillus niger* and the gene *ubiX* from *E. coli* were coexpressed in *E. coli,* the resulting decarboxylase enzyme ($Fdc1_{UbiX}$) displayed distinct spectral properties when compared to singly expressed Fdc1. $Fdc1_{UbiX}$ catalyzed the decarboxylation of multiple aromatic carboxylic acids *in vitro*[35], providing the first definitive evidence of dependent catalytic activity and the first indication that UbiD/Fdc1 are exclusively responsible for decarboxylation. The crystal structures of $Fdc1_{UbiX}$ using Fdc1 from *A. niger* (PDB CODE 4ZA4, 1.2 Å), *Camidida dubliensis* (PDB CODE 4ZAD, 2.5 Å) and *Sacchromyces cerevisiae* (PDB CODE 4ZAC, 1.7 Å) confirmed the identity of the prenylated flavin mononucleotide[35]. The crystal structures also revealed the presence of a metal ions in complex with the ribityl phosphate of the prenylated FMN, one of which was confirmed to be Mn^{2+} by EPR and the other is thought to be K^{+} [35, 46], consistent with early reports of the dependence of UbiX/Pad1 and UbiD/Fdc1 on Mn^{2+} [18].

The first crystal structure of UbiD from *E. coli* (PDB CODE 2IDB, 2.9 Å) was solved in 2006 by the Northeastern Structural Genomics Consortium and revealed a hexameric quaternary structure. However, due to the limited resolution of the data, specific details of residue identity and position could not be established. In 2013, a 1.9 Å-resolution crystal structure of the dimeric UbiD from *Psuedomonas aeurginosa* (PDB CODE 4IP2) was determined and the associated electron density maps displayed clear difference electron density indicative of a Mg^{2+} metal center[30]. A large cleft on the face of the structure extended from the metal binding site across 2 domains and terminated near a pocket of conserved residues Arg170, Glu273 and Glu278 that was designated as the putative active site. It was also noted that residues Glu229 and His188 from UbiD were structurally conserved with Glu105 and His68 in FMN-binding protein from *Methanobacterium thermoatuotrophicum*[47](PDB CODE 1EJE, 2.2 Å). These residues are believed

to be involved with the binding of flavin mononucleotide whose phosphate was bound to a similarly positioned metal ion. However, binding of FMN to UbiD could not be demonstrated by conventional methods[30].

Crystals of $Fdc1_{UbiX}$ from *A. niger* were soaked with various trans-cinnamic acid-related compounds: 4-vinyl guaiacol (PDB CODE 4ZAA, 1.2 Å), penta-fluorocinnamic acid (PDB CODE 4ZA8, 1.1 Å), phenylpyruvate (PDB CODE 4ZA9, 1.0 Å) and alpha-fluoro cinnamic acid (PDB CODE 4ZAB, 1.2 Å)[35]. The structures of these complexes indicate that the substrate's enoic acid double bond stacks directly above the oxidized prenylated flavin (prFMN) cofactor that was observed in two configurations, an isoalloxazine N5-iminium ($prFMN_{iminium}$) and an N5-ketamine species ($prFMN_{ketamine}$)[35] (Figure 3A & C).

UbiD and Fdc1 bind prenylated flavin mononucleotide in the reduced form ($prFMNH_2$) which then requires activation by oxidation to yield the iminium ($prFMN_{iminium}$) or possibly the ketamine ($prFMN_{ketamine}$) form[35] (Figure 3A & C). Conceivably, acid/base chemistry could utilize the N5 of the secondary ketamine as a catalyst, taking advantage of the positioning of the substrate's α,β-unsaturated carbonyl above the $prFMN_{ketamine}$-C4a to undergo Michael addition-like chemistry that has been observed in other flavin containing enzymes[48, 49], forming a transient C4a-substrate adduct prior to decarboxylation. The alternative would be to utilize $prFMN_{iminium}$ where the substrate α,β-unsaturated carbonyl, a dipolarophile, interacts with the 1,3-dipole arrangement of $prFMN_{iminium}$[50], to undergo what would be the first biological example of a 1,3 dipolar cycloaddition leading to the formation of a substrate-$prFMN_{iminium}$ adduct bridging both the C4a and C1' of the $prFMN_{iminium}$ cofactor (Figure 3). The bridged substrate-$prFMN_{iminium}$ could then undergo a Grob-like decarboxylation[51] of the pyrrolidine adduct that could be coupled to

cleavage of the C4a-substrate bond resulting in a prFMN-C1'-substrate adduct where protonation by Glu282 leads to the formation of the second double-bridged pyrrolidine adduct. This adduct would then be subject to retro 1,3-dipolar cycloaddition resulting in the formation of the product complex (Figure 3).

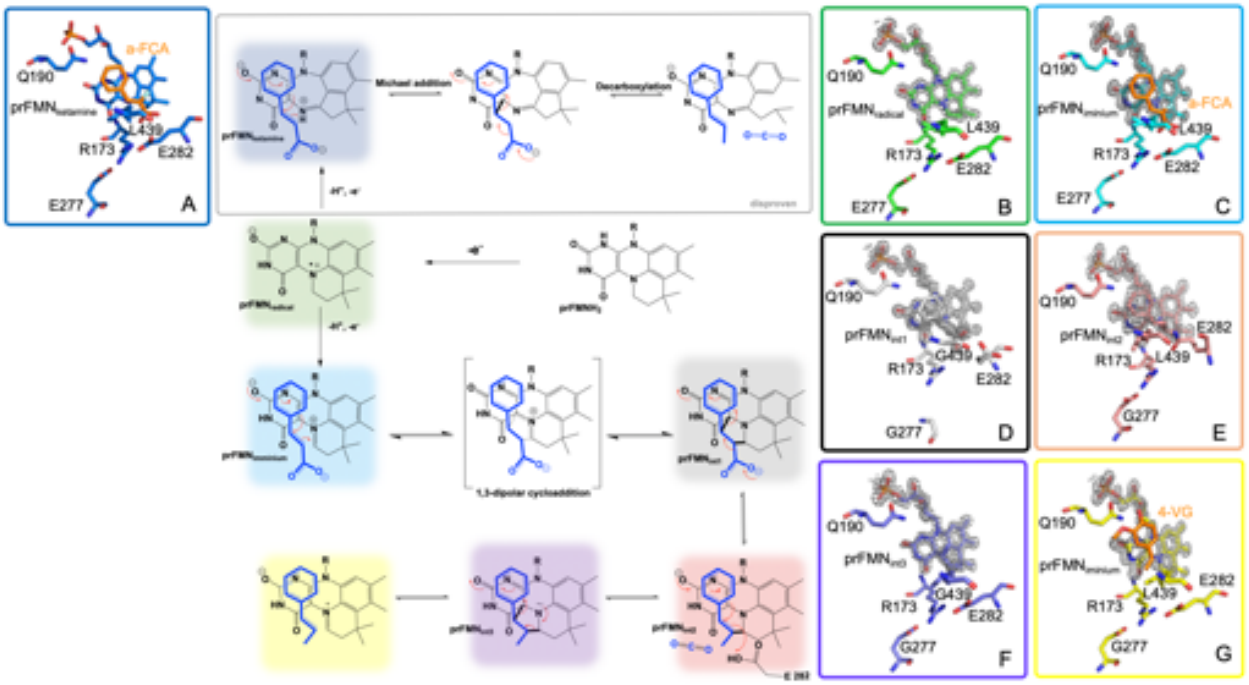

Figure 3. Proposed catalytic mechanism of $Fdc1_{UbiX}$ and supporting crystal structures of A. $prFMN_{ketamine}$•α-FCA (α-fluoro cinnamic acid) (PDB code 4ZAB), B. prFMNradical (PDB code 6R2T), C. prFMNiminium •α-FCA complex (PDB code 4ZAB), D. $prFMN_{int1}$ adduct (PDB code 6R3O), E. $prFMN_{int2}$ adduct (PDB code 6R3F), F. $prFMN_{int3}$ adduct (PDB code 6R3J) G. prFMNiminium •4-VG (4-vinyl glycol) complex (PDB code 4ZAA).

In an attempt to determine which pathway is utilized, $Fdc1_{UbiX}$ from *A. niger* was incubated with phenylpyruvate resulting in reversible inhibition of the enzyme by the enol tautomer. Crystal structures of this complex revealed the phenylacetaldehyde adduct with what would have been the imino form of prFMN. Moreover, crystallization in the presence of α-hydroxycinnamic acid indicated an α-hydroxystyrene prFMN-adduct, both confirming $prFMN_{iminium}$ as the active form of the enzyme[35]. Additional crystal structures of Fdc1 were solved in 2018 and 2019 and provided additional physical evidence in support of this mechanism in the

form of a structure of Fdc1•prenylated FMN in radical form and substrate analog phenylpropiolic acid (PDB code 6R2T, 1.3 Å) [52] (Figure 3B). Crystal structures representative of $prFMN_{int1}$ and $prFMN_{int2}$ were solved using L439G variant Fdc1 in the presence of phenylpropiolic acid (PDB code 6R30, 1.1 Å) and variant E282Q in the presence of cinnamic acid (PBD code 6R3F, 1.3 Å) respectively [53] (Figure 3D & E). Characterization of intermediate species was possible due to active site variant Fdc1, where L439G mutation resulted in a decrease in k_{cat} and a substantial increase in K_M and as a result the reaction ceased to undergo decarboxylation and confirmed the role of Phe437 in catalysis. Mutation of the glutamic acid responsible for the protonation[46] and E282Q abolishes catalysis with cinnamic acid and resulted in the formation of a distinct species determined to be intermediate 2 [53] (Figure 3E). Evidence for intermediate 3 was obtained from WT Fdc1 crystal structures that were flash-cooled proceeding exposure to cinnamic acid [53] (PDB code 6R3J) and revealed a prFMN crotonic acid adduct predicted to form after decarboxylation and protonation (Figure 3, F). The size and diverse nature of the crystal structure catalog and the formation of multiple dead-end complexes afforded from reactions with substrate analogs and/or variant forms of Fdc1 provide a composite of support for decarboxylation coupled to reversible 1,3 dipolar cycloaddition.

Kinetic insight into the mechanistic progression of $Fdc1_{UbiX}$ from *S. cerevisiae* where solvent and secondary deuterium isotope effects at the α and β positions of the phenylacrylic acid substrate support a mechanism involving 1,3 cycloaddition [54]. These observations indicate that carbon dioxide release is dependent on proton transfer to the product where proton transfer must precede the rate limiting step. The identification of the rate limiting step was determined from a linear free-energy analysis using a range of *para* and *meta*-substituted phenylacrylic acids

where Hammett parameters were consistent with formation of styrene via cyclo-elimination as rate limiting[54]. Additionally, reactions carried out in the presence of mechanism-based inhibitor 2-fluoro-2-nitro-vinylbenzene terminated with a cyclo-addition adduct and provide direct evidence that prFMN based chemistry proceeds via 1,3-dipolar cyclo-addition [55].

Covalent N5-iminium: UDP-galatopyranose mutase

UDP galactopyranose mutase (UGM) is a flavin dependent protein that catalyzes the 6- to 5-member sugar ring contraction of UDP-galactopyranose (UDP-galp) to form UDP-galactofuranose (UDP-galf). The reaction catalyzed transiently forms a covalent FAD-galp iminium complex intermediate necessary for nucleophilic attack and ring closure (Scheme 2). This reaction has an equilibrium position that favors UDP-galp (11:1) as a result of the increased ring strain generated in the contracted saccharide[56]. UGM is active in the reduced state of the flavin, the reaction is overall redox neutral and bifunctional in that it can recover the $FMNH_2$ after oxidation by acquiring electrons from NAD(P)H.

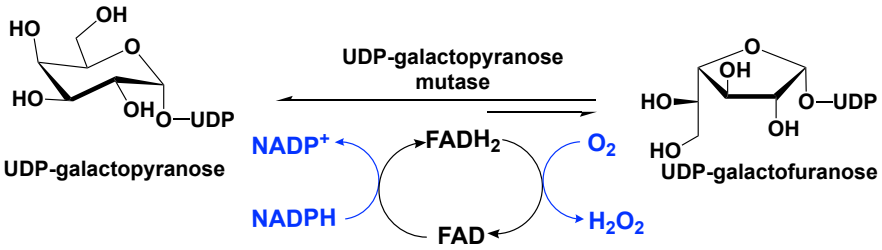

Scheme 2. Reaction catalyzed by UDP-galactopyranose mutase.

UDP-galf is a required precursor for the biosynthesis of galactofuranose-dependent glycoconjugates found in bacteria, fungi, and protists[57-60]. In mycobacteria species, UGM is responsible for the biosynthesis of precursors used for glycoconjugates that function in anchoring the outer mycolic acid layer to the peptidoglycan of the cell wall. Mutants of *Mycobacterium*

smegmatis that lack the gene *glf*, which codes for UGM, lacked the ability to grow at non-permissive temperatures confirming that UGM is essential for infective growth in these organisms[61]. UGM was also shown to have importance in the fungus *Aspergillus fumigatus,* the causative agent of aspergillosis that poses a lethal pulmonary threat to immunocompromised individuals[62]. Deletion of *glf* in *A. fumigatus* resulted in attenuated virulence in a low dose mouse model that was attributed to a decrease in the thickness of the cell wall resulting in an increased susceptibility to antifungal agents [63]. In kinetoplastids such as the protozoan species *Leishmania major* the monosaccharide product of UGM serves as a precursor for galactofuranose, which anchors lipophosphoglycans and glycoinositolphopholipids to the cytosolic surface of the cell[64]. Mutant *L. major* devoid of UGM activity paralleled growth of wild type species *in vitro* but displayed attenuated virulence[65]. These observations have spurred scientific investigation into the catalytic and structural characteristics of UGM in these organisms; this activity is absent in higher organisms, making UGM a target for anti-microbial, anti-fungal and anti-parasitic agents[61, 66]. As such, several recent studies have presented UGM inhibitor candidates with micromolar dissociation constants[67-72 73-76].

Initial reports indicated that UGM is FAD-dependent [56] and earlier reports had indicated that the oxidized form of the flavin is required for activity[77]. However, it was later determined that UGM is only active when the flavin is in the reduced form [78-83]. Eukaryotic UGMs from *A. fumigatus* and the protozoa *T. cruzi*, *L. Mexicana* and *L. infatum* utilize NADPH as a co-substrate and can both reinstate and stabilize the reduced form of the enzyme under aerobic conditions[84-86]. It was also demonstrated that once reduced, eukaryotic UGMs can complete an average of several hundred turnovers before oxidation/inactivation occurs. This behavior occurs as a result

of the rate of oxidation occurring 200 to 1500-fold slower than rate of re-reduction[85-87]. Bacterial UGM can also utilize NADPH for enzyme reactivation but requires a large excess of NADPH and extended incubation times due to a 10,000-fold slower reduction rate compared to eukaryotic UGM, suggesting that alternative physiological reductants may be utilized by the bacterial forms *in vivo*[88, 89]. Kinetic analysis demonstrated that UGM from *T. cruzi* and *A. fumigatus* undergo reduction of the flavin cofactor by NADH, 7- and 17-fold slower respectively than by NADPH but exhibit dissociation constants for NADH that are 5- and 10-fold lower than those for NADPH indicating no distinct preference in terms of k_{red}/K_d [87].

The most widely accepted chemical mechanism for UGM utilizes the flavin as a nucleophile to facilitate an attack on the anomeric carbon of the substrate displacing (but retaining) UDP. In this mechanism the binding of the substrate (UDP-galp) to reduced UGM results in a local reorganization of the active site resulting in positioning of the N5 of the FAD proximal (3.4 Å) to the C1-galp [85, 90-94]. This conformation facilitates a direct attack of the substrate anomeric carbon by the reduced flavin in a proposed S_N2-like mechanism[95] (Figure 4). Direct attack by the flavin was also supported by studies where substitution of FAD with 5-deaza-FAD resulted in inactive enzyme[96]. The results of 5-deaza-FAD substitution studies were initially proposed to be evidence in support of a mechanism involving single electron transfer[96], however the linear free energy relationship of k_{cat} to the nucleophilicity of the N5 position of UGM substituted with various flavin analogs resulted in a ρ value of -2.4, consistent only with a direct nucleophilic attack mechanism[97].

It is proposed that the nucleophilic attack of the FAD N5 of the reduced flavin UGM on the C1 of UDP-galp results in the formation of a covalent FAD-sugar adduct with the displacement

of the UDP (Figure 4, species 3/4). The formation of a covalent FAD reaction intermediate was confirmed in eukaryotic UGMs by UV/vis spectrophotometry and mass spectrometry[84]. The covalent FAD-galactose intermediate was also confirmed in prokaryotic UGMs by mass spectrometry, NMR and most recently by an X-ray crystal structure of *A. fumigatis (variant H63A)* (PDB CODE: 5HHF) (Figure 4, species 3, green)[93, 98, 99]. It was suggested that the sugar-FAD adduct would facilitate ring opening and activation of the C1 of galp where the flavin would act as a structural scaffold providing the dimensional constraints required for ring contraction[1, 87, 100, 101]. This mechanistic progression is also consistent with positional isotope exchange (PIX) studies that determined that the glycosidic bond of UDP-galp is cleaved during catalysis[77, 88]. The exact identity of the captured covalent sugar adduct in crystal structures from *A. fumigatus* could not be identified, however, researchers concluded it must be either species 3 or 4 of Figure 4 [98].

Kinetic studies conducted with UGM from *Trypanosoma cruzi* showed no evidence of the formation of a flavin semiquinone species during turnover[102] despite earlier reports suggesting the flavin semiquinone is stabilized by substrate binding[103]. Interestingly, these kinetic studies did reveal the formation of a possible flavin iminium ion intermediate (Figure 4, species 5)[84]. Hybrid quantum/classical calculations suggest that C4=O of the FAD accepts a proton from N5 of the FAD and subsequently donates it to the O5 of Galp[104]. FAD iminium ion formation would require deprotonation of the FAD N5 of the covalent FAD-sugar adduct, thereby facilitating opening of the ring of galp between C1 and the ether oxygen[87]. Hybrid simulations also predict that the proton for the C4-OH of Galp is shuttled to the C4=O of FAD during the contraction of the ring resulting in a covalent FAD-galf adduct[104]. To date there is no biochemical information

on the mechanisms of cleavage of the covalent FAD-galf complex or reconstruction of the galf-UDP molecule or the order in which they occur.

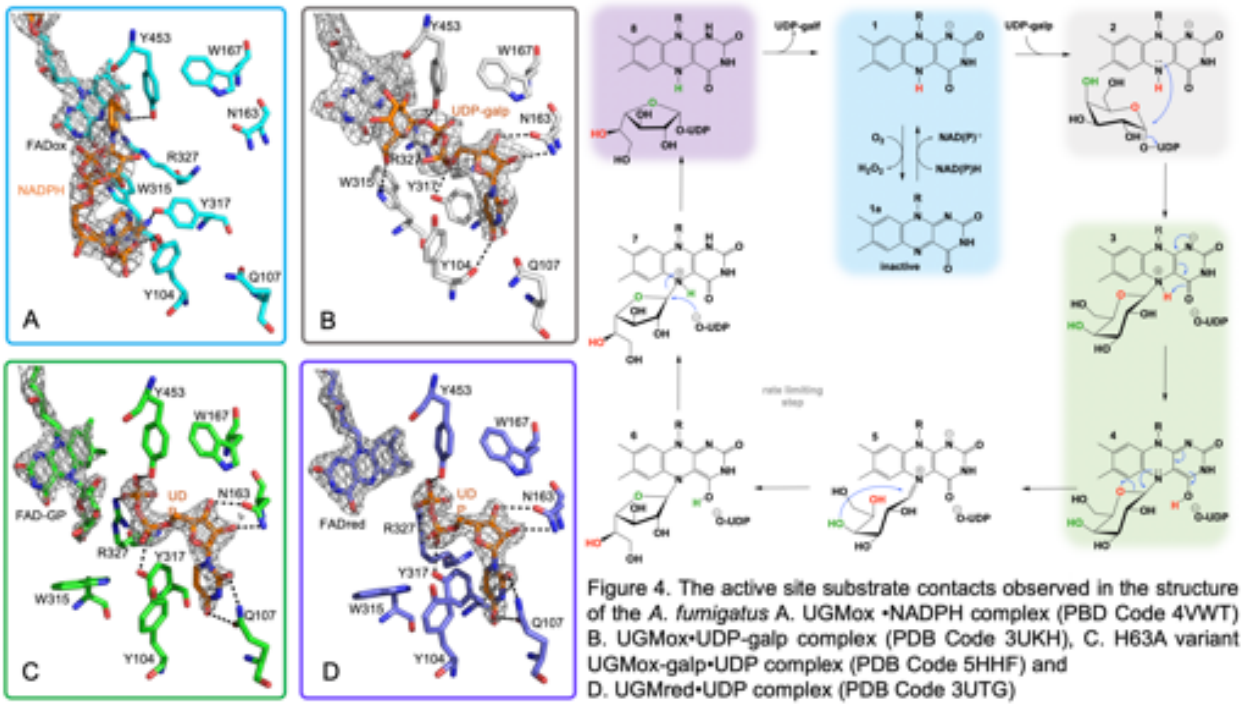

Figure 4. The active site substrate contacts observed in the structure of the *A. fumigatus* A. UGMox •NADPH complex (PBD Code 4VWT) B. UGMox•UDP-galp complex (PDB Code 3UKH), C. H63A variant UGMox-galp•UDP complex (PDB Code 5HHF) and D. UGMred•UDP complex (PDB Code 3UTG)

Kinetic analysis of UGM from *T. cruzi* demonstrated that the formation of the FAD iminium species occurs much more rapidly (300 s^{-1}) than the observed rate of catalysis (k_{cat} ~ 10 s^{-1}) and viscosity effects studies have ruled out product release as the rate-limiting step [84, 87]. On this basis, it was proposed that the rate of catalysis is governed by either the ring contraction or reattachment of UDP [84]. Additionally, studies on the rate limiting step in UGM from *A. fumigatis* recorded kinetic isotope effects of ~2 during the conversion of UPD-galp/galf and solvent viscosity effects suggesting that slow proton transfer dictates the rate limiting step and that product release is only partially rate limiting[101]. This study also determined that structural recognition of the hydroxymethyl group of the hexose C5 provides a kinetic barrier to cyclization and mutation of tryptophan 315 to alanine results in a 370-fold decrease in k_{cat}/K_M compared to

wildtype UGM where in the variant product release describes k_{cat} and that effect could be mimicked in wildtype UGM when utilizing UDP-arabinopyranose as a substrate[101].

The three-dimensional structure of UGM has been extensively characterized and revealed a complex topology consisting of three domains[80]. The structure of domain one is non-contiguous containing an abbreviated Rossman fold responsible for FAD binding, however, UGM from *E. coli* lacks the terminal strand of the Rossman fold [105]. Domain 2 is contiguous and includes a cluster of five α-helices that form the binding site for the uridine group, the active site "flap 1" (residues 167 to 177 in *K. pneumoniae* UGM) that undergoes UDP-galp dependent conformational changes and has a role in dimerization[106]. The third domain is non-contiguous and consists of a 6-stranded antiparallel β-sheet. The structures of all bacterial UGMs are topologically similar where secondary-structure matching analysis revealed that 73-96 % of secondary structure elements found in UGM from *E. coli* are completely conserved across all other known bacterial UGMs [107] despite substantial variation in primary structure (37-44 % pairwise identity with UGM from *E. coli*)[87].

In all, 59 structures of UGM from 9 different species including prokaryotic strains from; *Camplobacter jejuni, Corynebacterium diphtheriae, Dienococcus radiodurans, Mycolicibacterium smegmatis, Klebsiella pnuemoniae, Mycobacterium tuberculosis* and *Escherichia coli* as well as examples from the eukaryotes *A. fumigatus* and *T. cruzi* have been solved[67, 80, 85, 87, 91-94, 99, 102, 106, 108-111]. These structures included examples of UGM in both the oxidized and reduced states and in complex with multiple ligands including NADH, NADPH, flavin mononucleotide (FMN), UDP-phosphono-galactopyranose, UDP-galactose, UDP, UDP-galp and dideoxy-tetrafluorinated analogs, both the substrate and product, UDP-F_4-galp and UDP-F_4-galf as well as the potential

inhibitor 2-[4-(4-chlorophenyl)-7-(2-thienyl)-2-thia-5,6,8,9-tetrabicyclo[4.3.0]nona-4,7,9-trien-3-yl]acetate [67, 90, 91, 93, 94, 99, 102, 106, 109]. Single site directed variant UGM structures of Phe66Ala, Tyr317Ala, Asn207Ala, Gln107Ala, Tyr104Ala and His63Ala variants of the *A. fumigatus* UGM have also been determined [87, 92, 110, 111]. Possibly the most directly edifying structures with regard to the UDP-galp chemistry are the UGM_{red}•$NADP^+$ (PDB code 4VWT, 2.8Å), UGM_{red}•UDP (PDB code 3UTG, 2.3 Å), UGM_{ox}•UDP-galp (PDB code 3UKH, 2.3Å) and the covalent UGM_{ox}-galp•UDP (PDB code 5HHF, 2.3Å) crystal structure complexes depicted in Figure 4.

Multiple challenges in structure determination were encountered for UGM from eukaryotic species, *A. fumigatus*[90, 109, 112] and *L. major*[91], including translational pseudo-symmetry and crystal twinning. It was ultimately determined that mutagenesis of long-chain charged surface residues, specifically lysine and glutamine allowed for reproducible growth of crystals that were free of crystallographic pathologies [109, 113, 114]. Two independent groups solved the variant crystal structures of UGM from *A. fumigatus* using either the double variant Lys344Ala/Lys345Ala[109] or the single variant Arg327Ala[90] and the two structures produced are almost identical. These structures revealed that eukaryotic UGM consists of three domains similar to UGMs from prokaryotes with noticeable variations. Domain one retains the shortened Rossman-fold described for prokaryotic UGMs but has an additional 4-stranded antiparrellel β-sheet that sits adjacent to the Rossman fold and an extended ~30 residue C-terminus that plays a role in the tetrameric assembly of UGM from *A. fumigatus*. Domain two consists of a bundle of α-helices similar to prokaryotic enzymes but contains an additional α-helix and a helical extension (~7 residues), which are involved in tetramer formation. The additional α-helix forms the scaffold for a mobile active site ”flap 2” absent in prokaryotic UGMs. Domain three contains a twisted,

seven-stranded antiparallel β-sheet compared to the six-stranded β-sheet seen in prokaryotes. More recently the crystal structure of UGM from *T. cruzi* was solved in both oxidized (PDB code 4DSG) and reduced (PDB code 4DSH) states[102]. The protomer structure was highly similar to *A. fumigatus* (RMSD 1.1 Å)[87], though UGM from *T. cruzi* crystallized as a monomer as opposed to the homotetramer, consistent with results of small angle X-ray scattering[102].

Additionally, crystal structures of eukaryotic UGM from *A. fumigatus* were solved in complex with NADH (2.8 Å, PDB code 4GDD) and NADPH (2.8 Å, PDB code 4GDC) and have provided a valuable description of the unique NAD(P)H binding site[85]. The NAD(P)H molecule is sandwiched between domain one and three, forming interactions with both and is positioned in an unusually constrained conformation that positions the adenine moiety within hydrogen bonding distance of the ribose hydroxyl[111], an arrangement that is wholly different than the Rossman dinucleotide-binding fold described for most enzymes that utilize NAD(P)H as a substrate [115, 116]. Multiple conserved residues (Asn57, Ile65, Phe66, His68, Arg91, Ser93, Tyr104 and Tyr317) are involved in stabilizing the E•NAD(P)H complex where hydrogen bonding between Tyr104 and the 2' phosphoryl group of NADPH is responsible for the ~180-fold preference (k_{cat}/K_D) for NADPH over NADH seen in UGM from *A. fumigatus*[109]. However, binding of NAD(P)H molecules does not induce conformational changes in either of the two dynamic active site flaps (residues 179 to 187 and residues 203 to 209) responsible for access to the active site[109]. Interestingly, the bound NAD(P)H molecule extends into the UPD-galp binding pocket and implies that binding of NAD(P)H and UDP-galp are mutually exclusive[87]. Prokaryotic UGM lacks all of the conserved residues that contact the ADPP moiety of NADPH seen in eukaryotic UGM indicating

that prokaryotic UGM does not contain a recognizable NADPH binding domain which is consistent with biochemical data[87].

EncM

Flavins have been regarded as participating in a well-defined set of reaction categories [1, 117-120]. Flavin-dependent monooxygenases were thought to almost exclusively stabilize a C4a-(hydro)peroxyflavin intermediate as the oxygenating entity[117, 121-124]. In 2013, a unique bacterial enzyme, EncM, was described. This enzyme catalyzed the C4a-peroxyflavin independent oxygenation and dehydrogenation of a poly(β-carbonyl) substrate, promoting a Favorskii-like rearrangement to form desmethyl-5-deoxyenterocin which is then further transformed by enzymes EncK and EncR to form the antibacterial enterocin (Scheme 3). EncM was ultimately found to utilize a covalent flavin-N5-oxide as the oxygenating species[125, 126]. This highly unusual species is the first example of a four-electron oxidized flavin cofactor[125].

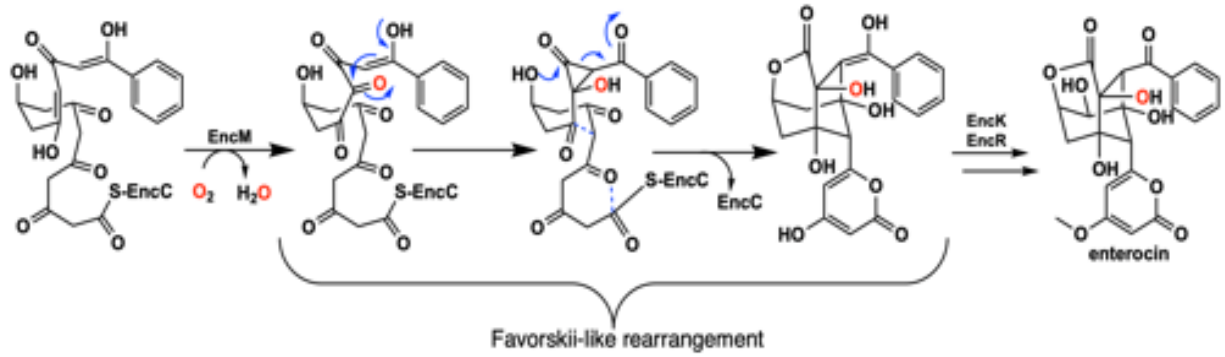

Scheme 3. The reaction catalyzed by EncM and subsequent conversion to enterocin by EncK and EncR.

EncM functions in the biosynthesis of enterocin in multiple streptomycete bacteria [127-130]. Dual oxidation reactions of the otherwise promiscuously reactive poly(β-carbonyl) substrate promote the Favorskii-type rearrangement resulting in the formation of the cyclohexanyl and

lactam rings of enterocin[125, 131]. The first crystal structure of unliganded EncM was published in 2013 (PDB code 3W8W, 2.0 Å) along with a structure determined in the presence of NADPH (PDB code 4XLO, 1.7 Å, *vide infra*). These structures revealed that, consistent with quaternary structure determinations, EncM crystallizes as a homodimer [125]. The structures also showed that residues 2-210 and 419-461 form an FAD-binding domain where covalent binding of the C8-methyl of the isoalloxazine moiety to His78, positions the flavin isoalloxazine moiety adjacent to the substrate-binding domain where it forms one internal face of the active site (Figure 5). The active site is adjacent to a group of positively charged residues at the protein's surface that form a basic region that is complementary in charge and shape to the negative surface of the EncC carrier protein (Scheme 3)[130, 132].

On this basis it was proposed that this electrostatic surface complementarity enhances protein-protein interaction between the polyketide carrier protein, EncC and EncM, limiting deleterious side reactivity of the substrate poly(β-carbonyl) chain [125, 127]. Additionally, mutagenesis studies designed to disrupt this protein-protein interface resulted in a ~40% decrease in activity compared to wild type [125]. Additional crystal structures of EncM where solved in complex with the substrate analogs: trifluorotriketide (PDB code 3W8X, 1.8 Å) and hydroxytetraketide (PDB code 3W8Z, 1.8 Å) [125](Figure 5A & C). These structures indicate that the terminal benzene group forms multiple van der Waals and π-stacking interactions with hydrophobic residues of EncM. These interactions position the enol proximal to the C1 of the substrate analog(s) within hydrogen bonding distance (2.4 Å) of the O(4) of the flavin. The key active site residues lie on the terminal limb of an L-shaped tunnel ~30 Å in length that extends to the surface of the enzyme near the dimer interface. The shape of this tunnel is complementary

to an open conformation of the acyl carrier protein bonded phosphopantetheine arm and the ketide chain of the 1,3-diketone substrate, whose presumed function is to physically separate the phenyl-tetraketide head from the remaining tetraketide tail and suppress adventitious cyclization/aromatization reactions[125].

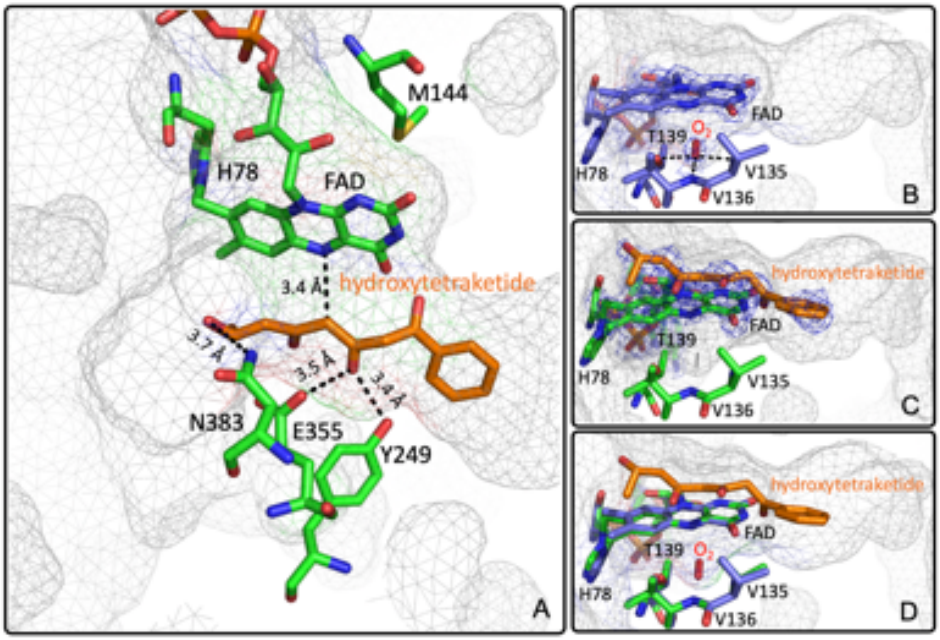

Figure 5. The Active Site of EncM. Left. A. EncM with a hydroxytriketide substrate analogue bound (PDB code 3W8Z). Right (top to bottom). B. EncM crystalized in the presence of 15 bar dioxygen (PDB code 6FOQ), C. EncM in complex with a hydroxytriketide substrate analogue bound (PDB code 3W8Z) and D. overlay of both structures. The mesh indicates the shape of the terminal end of the internal cavity. Electron density is shown in blue and derived from 2fo-fc maps or associated structure files.

Interestingly, the active form of EncM has a spectrum that closely resembles that of two-electron oxidized flavin. The enzyme is observed to inactivate after an average of only seven turnovers and this results in a blue shift and an increase in the extinction coefficient of the isoalloxazine absorption transitions[126]. It was proposed that inactivation resulted from the loss of the flavin oxygenating species[125, 126]. Reactivation was observed in the presence of NAD(P)H and dioxygen. While, EncM does not have a catalytic requirement for NAD(P)H and lacks a conventional nicotinamide dinucleotide binding domain, it does appear that NAD(P)H has a biological role in reactivation of the enzyme [126] by returning the flavin to the reduced resting state (~0.100 s^{-1}) from where a reaction with dioxygen can (re)form the flavin N5-O oxygenating

intermediate. This proposal is supported by data that describes ~36-fold lower binding affinity for NADPH compared to NADH while maintaining similar limiting rate constant for flavin reduction (~0.100 s^{-1}) [126]. Despite efforts, no structural evidence has been offered for the EncM •NADPH complex [126].

As mentioned above, conventional flavin monooxygenase chemistry utilizes a flavin-C4a-(hydro)peroxide[122, 133, 134] to oxygenate target substrates. For EncM this intermediate was readily ruled out by the UV-Vis spectral characteristics. It was also observed that the generation of the EncM flavin oxygenating species from anaerobically reduced enzyme required dioxygen; anoxic chemical reoxidation resulted in oxidized inactive enzyme[125]. Additionally, when EncM that was reoxidized with $^{18}O_2$ and reacted with a truncated racemic substrate, there was a 1:1 conversion to a diastereomeric mixture of products that were identified by NMR and MS as the ring-open derivatives of the predicted lactone[125]. These studies also revealed that the substrate-binding tunnel of EncM is specifically tailored to accommodate only the C7-(R)-enantiomer of the substrate, supporting the observed single configuration of the C4-hydroxyl in the enterocin product[125]. Based on these observations the EncM oxygenating species was proposed to be the flavin-N5-oxide formed from a reaction of the reduced enzyme with dioxygen[125, 135, 136]. More direct evidence for the active N5-oxide flavin came in 2015 when researchers analyzed peptide fragments generated proteinase K digestion of EncM using LCMS and identified a mass consistent with the predicted His78-bound flavin N5-oxide fragment[126]. To definitively correlate the observed mass signal with the flavin-bonded oxygen molecule, chemically reduced EncM was reoxidized by $^{18}O_2$ and $^{16}O_2$ and then analyzed similarly by LCMS to confirm the generation of a masses consistent with a flavin-N5 isotopic incorporation[126].

Extensive investigation into the mechanism and control of oxygen reactivity mediated by EncM has led to a better understanding of these unique enzymatic events[126, 137]. Reaction of the reduced enzyme with dioxygen was originally proposed[126] to involve the reduced flavin reacting conventionally with dioxygen resulting in a flavin-C4a-hydroperoxide that immediately undergoes water elimination to form an epoxide that is then opened to form the flavin-N5-oxoammonium/N5-oxide (Scheme 4, top). However, the orientation of the predicted C4a-peroxide would disfavor formation of the ring-strained oxaziridine and on this basis this mechanism has been replaced by a radical coupling mechanism (Scheme 4, bottom)[126]. This mechanism is defined by direct proton transfer between flavin N5 and dioxygen resulting in the formation of a protonated superoxide (peroxyl radical) and an anionic semiquinone which subsequently dehydrates to form the N5-oxoammonium/N5-oxo resonance pair. Stabilization of the flavin anionic semiquinone by EncM[125] would promote the reaction with the protonated superoxide as a consequence of high spin density at the N5 [138, 139]. Additionally, oxidation of reduced EncM by dioxygen occurred without the formation of detectable intermediates[137]. These experiments also demonstrated that the observed rate constants titrate to a saturating dioxygen concentration and support a two-step mechanism with a binding event preceding adduct formation[137].

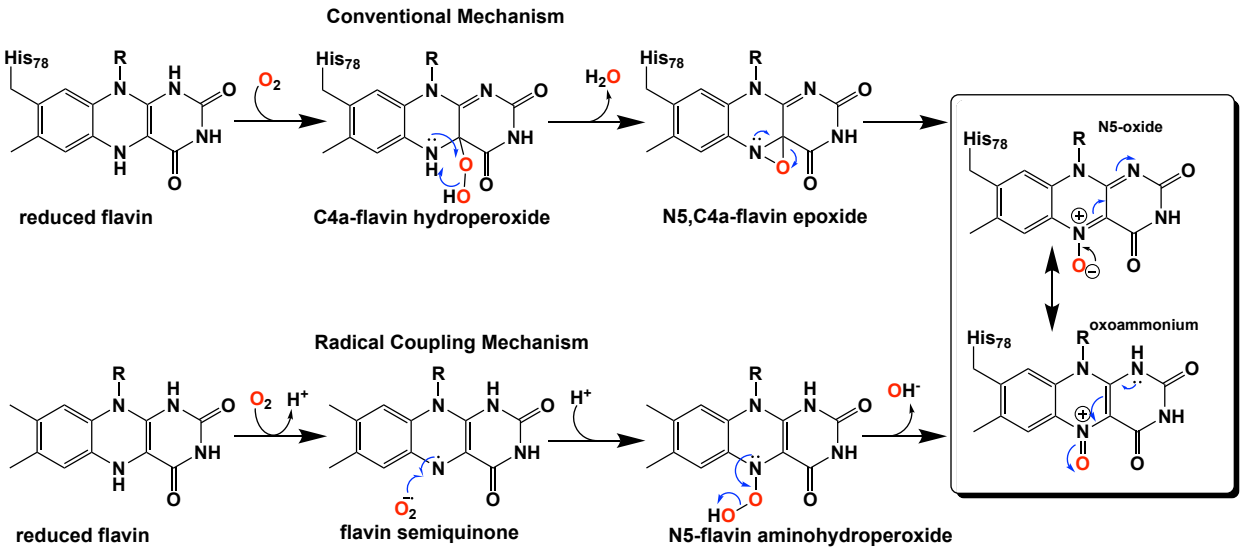

Scheme 4. Proposed pathways for the formation of the flavin N(5)-oxide

Direct structural insights for dioxygen reactivity were obtained from pressurized-dioxygen X-ray crystallography which exposed crystallized EncM to controlled pressures of oxygen. These structures displayed significant electron density proximal to the *re*-face of the isoalloxazine moiety and adjacent to the amphiphilic pocket previously identified[125] not seen in either anaerobic or noble gas controls (Figure 5B & D) [137]. A definitive oblong shape was observed in the omit map was proximal to three residues (V135, V136 and T139) within 3 Å of the observed density. These residues were assumed to be required for appropriate positioning for short range electron transfer to the flavin N5[137]. Curiously, many of the structures obtained in this study had no electron density indicative of flavinylation between H78 and the C8a of the isoalloxazine moiety of FAD as was observed in prior structures[137].

Mutational analysis of the residues that form the suspected dioxygen binding pocket largely destabilized the enzyme and mutation of adjacent residues (L144, L116, H138 and L117) resulted in diminshed dioxygen occupancy of crystal structures and impeded catalysis and in one

instance (T139V) oxidase activity was observed[137]. It is likely this activity parallels previous observations of EncM inactivation, where atmospheric dioxygen aberrantly oxidizes the bound diketone to the triketone mimicking conventional turnover. This further supports a route of reactivation via flavin reduction and subsequent reaction with dioxygen to form the N5-oxide. Furthermore it also suggests that kinetic inactivation may be a function of truncated substrate analogs that do not fully preclude adventitious reaction by dioxygen.

Due to the intramolecular reactivity, preparation of the native substrate is difficult and analogs with truncated ketide chains have been used to study EncM[125]. The mechanism proposed from studies with these substrates is depicted in Scheme 5. In this mechanism, the oxoammonium of the flavin undergoes attack by the proximal enolate of the substrate, resulting in the formation of amine-oxo-bridged species. This is cleaved by protonation yielding the flavin cofactor and generation of a C4-hydroxylated intermediate. Hydride transfer to the flavin produces the C4-ketone product and the reduced form of the flavin cofactor.

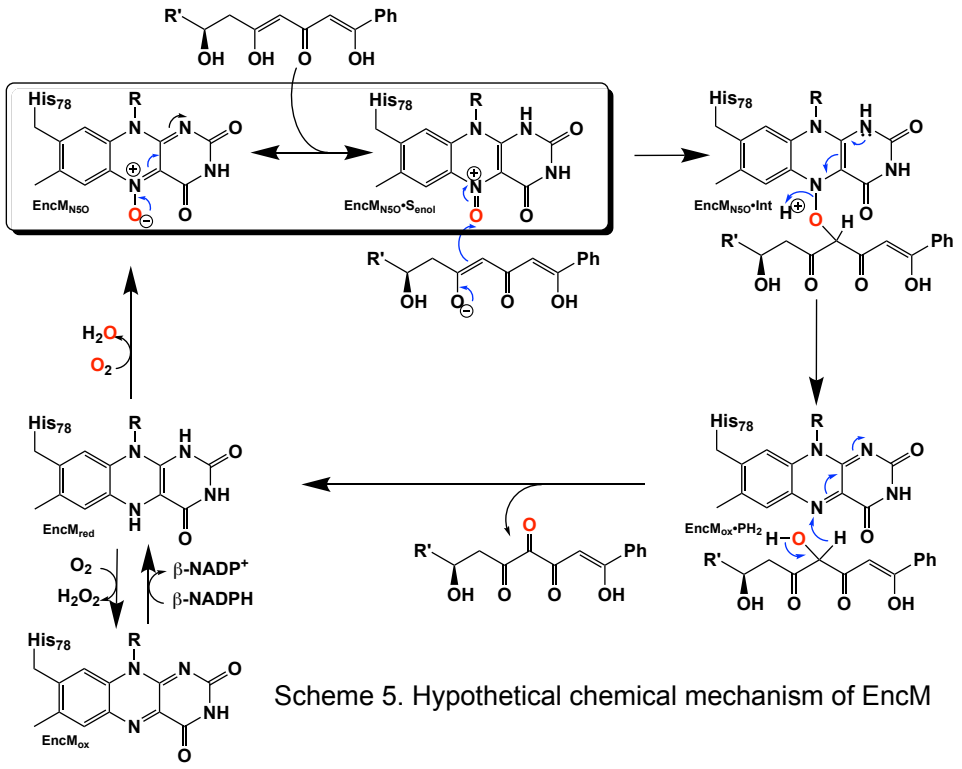

Scheme 5. Hypothetical chemical mechanism of EncM

EncM presents the first example of a flavoprotein that requires a hyperoxidized flavin cofactor (flavin-N5-oxide) for its catalytic function. This discovery prompts the question, given the similarity of the spectra of the flavin N5-oxide and two-electron oxidized flavin, is EncM an unusual flavoprotein that displays unique chemistry or is this just the first identified of a new class of enzymes?

RutA

The discovery of the flavin N5-oxide, whose spectrum closely resembles that of two-electron oxidized flavin has prompted scrutiny of previous investigations of flavo-enzymes that exhibit unique oxygenation chemistries. The objective was to ascertain if the flavin-N5-oxide is common or idiosyncratic. This inquiry has yielded the discovery a class of enzymes that catalyze the oxygenated cleavage of a diverse set of substrates by the enzymes RutA, DszA and HbcA1

that each utilize a flavin-N5-oxide [52, 140, 141] (Scheme 6). It is of note that this newly described class of enzymes contains FMN and not an FAD as in the case of EncM. We will focus on the enzyme RutA as the hallmark example, which catalyzes the amide cleavage and oxygenation of uracil and thymine to form 3-ureidoacrylate or 2-methylureidoacrylate respectively[142].

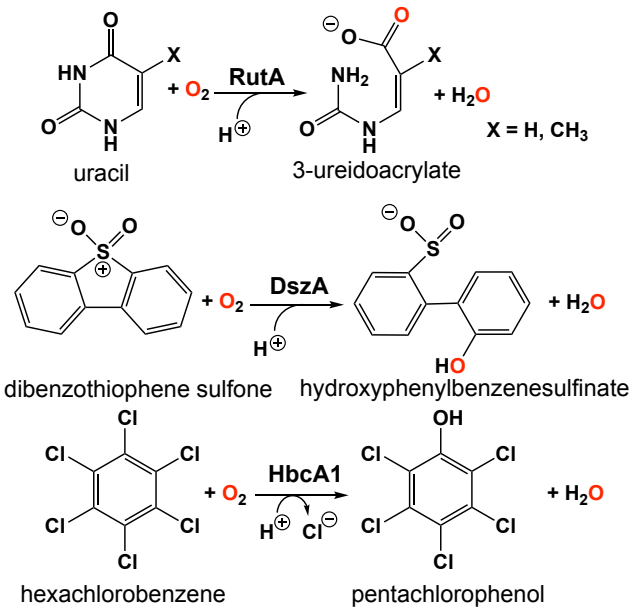

Scheme 6. Reactions catalyzed by N5 mediated monooxygenation enzymes; RutA, DszA and HbcA1.

It was the long standing notion that pyrimidines thymine and uracil were exclusively catabolized by one of two pathways described as oxidative or reductive[143]. The reductive pathway is well described and is expressed in a diversity of organisms including archaea, bacteria and eukaryotes [144-146]. This pathway follows NAD(P)H dependent catabolism of uracil or thymine to yield carbon dioxide, ammonia and either β-alanine (uracil) or β-aminoisobutyrate (thymine). The oxidative pathway is confined to a variety of bacteria and affords urea and either malonic acid (uracil) or methylmalonic acid (thymine) as products [147, 148]. However, in 2006 Loh et al described an additional pathway of pyrimidine catabolism encoded by the b1012 operon of *E coli* K-12. This novel third pathway relies on reducing equivalents from NAD(P)H to yield 3-

hydroxypropionic acid (uracil) or 2-methyl-3-hydroxypropionic acid (thymine), carbon dioxide and ammonia[149] (Scheme 6). The discovery of RutA was a result of analysis of a strain of *E. coli* carrying the ntrB(Con) mutation that can utilize thymidine as the sole nitrogen source and lesions in the b1012 operon completely nullified this activity[149]. These researchers also characterized the gene products of this operon as encoding a seven-enzyme system tentatively including, endoribonuclease (RutC), nitroreductase (RutE), flavin reductase (RutF), xanthine/uracil permease (RutG), punitive isochorismatase (RutB), punative α/β hydrolase (RutD) and a monooxygenase (RutA).

The initial step of the Rut pyrimidine catabolism pathway was originally described as a "oxidative hydrolysis" of uracil to yield 3-ureidoacrylate. It was quickly determined that this activity is catalyzed by RutA and RutF in the presence of FMN and NADH, where the presence of a flavin reductase (RutF) was required to reduce and transfer a flavin to RutA[142]. The formation of 3-ureidoacrylate was determined in these reactions by HPLC and cleavage of the N3-C4 bond was confirmed by ^{13}C NMR in reactions utilizing ^{13}C,^{15}N-labeled uracil[142]. These results led researchers to propose a catalytic mechanism consistent known flavin oxygenations that utilize a C4a-centered oxygenation and a subsequent reduction reaction (Scheme 7, blue). Initially it was unclear whether the acquisition of pyrimidine substrate was dependent on the presence or redox state of FMN. Only the RutA•pyr•$FMNH_2$ complex can undergo a reaction with dioxygen to transiently form the peroxyflavin species that facilitates the nucleophilic attack of the C4 of the pyrimidine resulting in ring cleavage. Though this mechanism is based on scientific precedent it does not describe the source of reducing equivalents for conversion of the predicted 3-ureidoacrylic peracid species. It was concluded that reduction must be either adventitious/non-

catalytic or accomplished by a separate enzyme[142]. Furthermore, early crystal structures of RutA solved in the presence of uracil (PDB code 5WAN, 1.8 Å) (Figure 6) revealed an overall structure typical of group C FMN dependent flavin monooxygenases[150] but did not contain an active site cysteine residue previously shown to stabilize the flavin C4a-hydroperoxide [151].

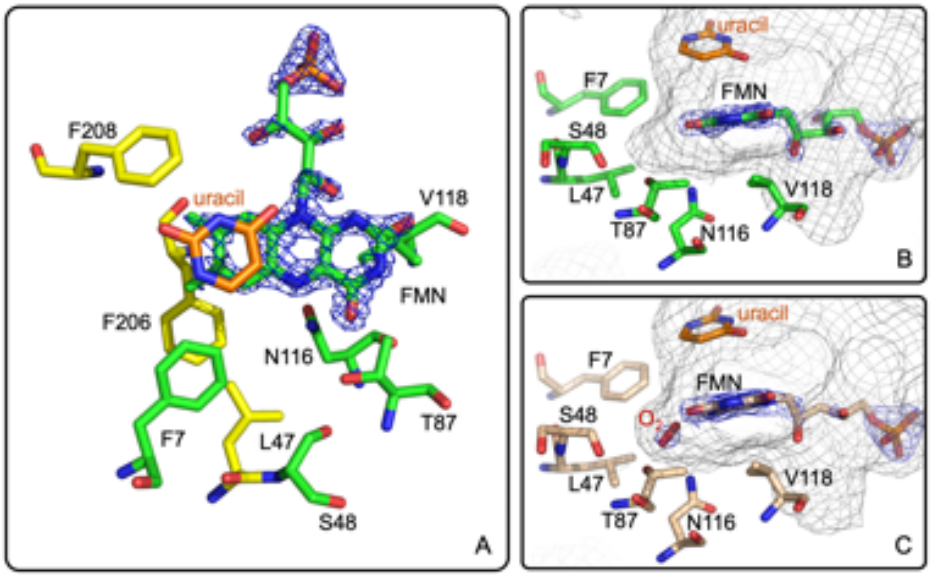

Figure 6. The active site of RutA. A & B. RutA in complex with uracil substrate bound (PDB code 5WAN). Active site residues that are involved in N5-oxo formation are shown in green. (C) Active site of RutA in complex with uracil under 15 bar dioxygen (PDB code 6TEG). Electron density is shown in blue mesh and the active site cavity is shown in grey mesh.

It is unclear specifically what led these researchers to revisit their initial mechanistic rationale, but seven years subsequent to their initial proposal a new mechanism was offered[141] (Scheme 7, green). The mechanistic amendment was a result of heat quench experiments that anaerobically reacted photo-reduced RutA with stoichiometric amounts of uracil which resulted in the formation of a stabile flavin-N5-oxide as determine by LC-MS and HPLC coelution with a synthesized flavin-N5-oxide[141]. Furthermore, a repeat of the aforementioned reaction carried out in the presence of $^{18}O_2$ resulted in a 2 Da mass shift consistent with the incorporation of a single oxygen atom from molecular oxygen. Overall this mechanism parallels that of the original proposal where C4a oxygen activation catalyzes the cleavage of the 3,4-amide linkage of the pyrimidine, but terminates instead at a product elimination step that affords a flavin N5-oxide

coupled to the cleavage of 3-ureidoacrylic peracid. Included is a second role for RutF, reinstating the reduced flavin in place of the N5-oxide.

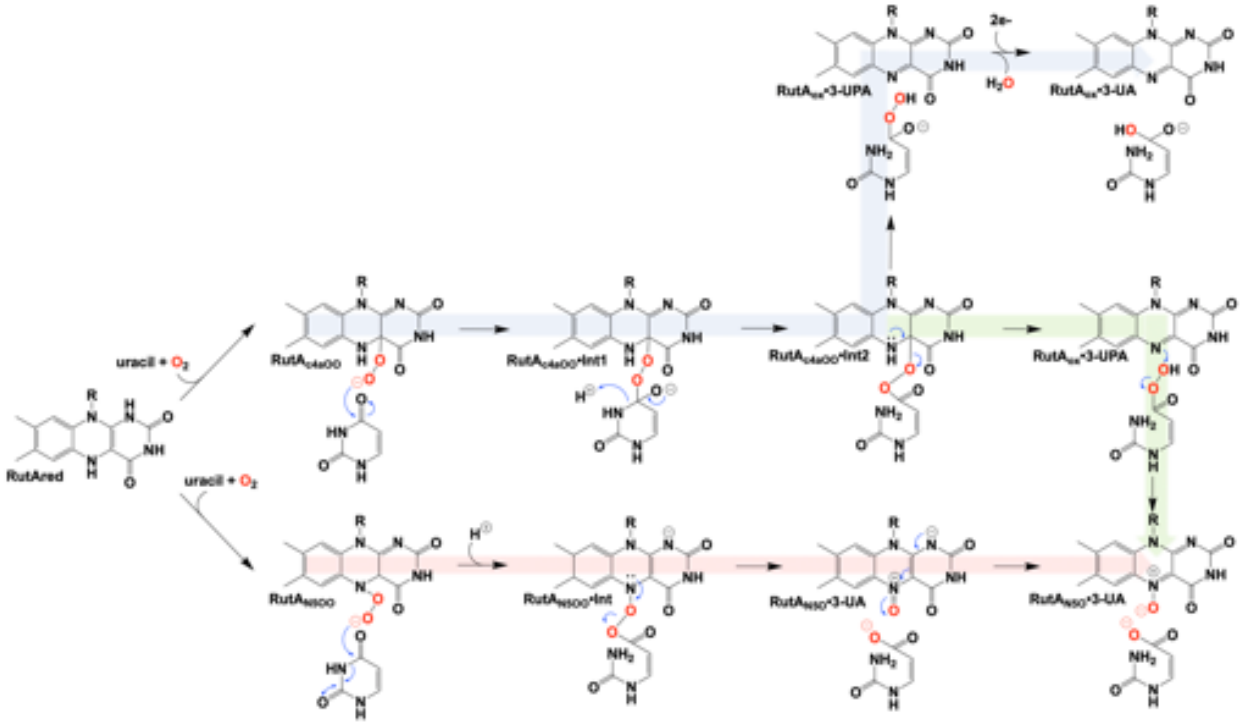

Scheme 7. Proposed chemical mechanisms of RutA. Blue, initial mechanism utilizing a C4a-hydroperoxyl. Green, mechanism terminating in the formation of an N(5)-oxide complex. Red, direct oxygen transfer mechanism utilizing an N(5)-hydroperoxide and terminating with the formation of an N(5)-oxide complex.

Further insight into the catalytic mechanism of RutA came in 2020 when a group of researchers obtained crystal structures of oxidized RutA in the presence of non-convertible substrate analogs 4-thiouracil (PDB code 6SGM, 2.0 Å) and 2,4-dimethoxypyrimidine (PDB code 6SGN, 2.5 Å) [152]. These crystal structures confirmed the existence of a ligand binding pocket adjacent to the *si*-face of the isoalloxazine moiety (Figure 6) [153, 154]. Surprisingly, very few side chain interactions exist between the bound pyrimidine and RutA despite prior evidence that flavin-N5 formation is predicated on substrate association[141]. Furthermore, ligand association did not result in any obvious changes to the protein scaffold. These structures also revealed the presence of a second, more confined (~24 Å^3) active site cavity lined with nonpolar side chains

(L65, V136, and F224) proximal the substrate binding pocket that is necessary to bind the hydrophobic dioxygen molecule (Figure 6, grey mesh). The distal portion of the presumed dioxygen binding pocket is occupied by the polar side chains of T105 and N134 and likely stabilizes the hydrophilic protonated superoxide through hydrogen bonding. Mutational analysis of residues T105, N134 and V136 that line the putative dioxygen binding cavity abolished activity except in the case of T105S which retained ~80% of WT activity[141]. The absolute requirement of the positioning and identity of amino acid residues involved coupled with the confined nature of active cavity (radius ~1.8 Å compared to the anisotropic Van der Waals radii of gaseous dioxygen of 1.77) highlights that proper dioxygen positioning is fundamental to catalysis[152].

Aside from traditional C4a-flavin oxygenase enzymes, dioxygen reactivity of flavoproteins is most commonly bimolecular and does not involve a prior complex[118, 137, 155, 156]. To confirm the existence of an *bona fide* oxygen binding pocket, O_2-pressurized X-ray crystallography was used to expose crystals to varying pressures of dioxygen from 0 to 15 bar immediately preceding freezing in liquid nitrogen[152]. Significant electron densities not seen in anaerobic controls was observed adjacent to the *si*-face of the flavin in all crystals exposed to dioxygen prior to diffraction and the intensity of the electron density titrated with increased oxygen pressures of 0 bar (PDB code 6TEE, 2.2 Å) 5 bar (PDB code 6TEF, 1.8 Å) and 15 bar (PDB code 6SGG, 1.8 Å). Modelled dioxygen conforms well to the observed electron densities generated from 2fo-fc maps (PDB code 6TEG, 1.9 Å) (Figure 6, C). The protein therefore directs the proximal oxygen atom to localize ~2.1 Å from the flavin-N5, indicative of a direct interaction with this position and significantly closer than the distance to the flavin-C4a (3.1 Å). Furthermore, the angle between the modelled

dioxygen the flavin-N5 is 99 °, while the angle to the flavin-C4a position is 118°, predicting the former as the preferred point of reaction.

In 2020 Matthews et al added another mechanistic addendum to the proposed mechanism of RutA (Scheme 7, red)[152]. The mechanism proposed initiates with the formation of the flavin-N5-oxide generated from the RutA•$FMNH_2$ complex via a radical coupling mechanism as described for EncM (Scheme 4). This is a deviation from the initially proposed mechanisms that form such a species concomitant with product release[141]. This modification is supported by HPLC and LCMS analysis that confirm the formation of flavin-N5-oxide in reactions carried out in the presence of both convertible and nonconvertible substrate analogs (2-thiouracil, 4-thiouracil, 2,4-dithiouracil, DMP, cytosine, and 1,3-cyclohexanedione)[152]. Despite the formation of active flavin-N5-oxide with all analogs tested, HPLC analysis of these reactions confirmed only 2-thiouracil was able to illicit catalysis[152] and confirmed the absolute requirement of the presence of a pyrimidine substrate with an intact amide moiety for turnover. Establishment of this initial oxygenating species would then predict that the actual identity of the oxygenating species is the flavin-N5-peroxide and not the flavin-C4a-peroxide (Scheme 7). As such, the neutral N5-peroxide would act as a soft nucleophile promoting an umbrella/nitrogen inversion abridging the distance to the substrate amide for cleavage and subsequent direct/covalent oxygenation forming 3-UA and the flavin N5-oxide.

The discovery of a third flavin oxygenating species unique from flavin-C4a and recently discovered flavin N5-oxide, provides for a redox neutral oxygenative cleavage. This discovery convincingly describes the existence of a new oxygenating class of flavoproteins, unique in both mechanism and scaffold, that utilize the electron donating properties of the hyperoxidized

isoalloxazine to accomplish a unique net transfer of a hydroxide. To date three examples of such chemistry have been described and provide an identifiable motif that is found in a number of oxygenase enzyme primary sequences[152]. These results, in part, suggest that reinterpretation of previously described group C monooxygenases could provide additional examples of N5 oxygenative chemistries that have been dogmatically assigned as C4a centered oxygenation.

Conclusive Remarks

The involvement of the flavin N5 position in enzymatic reactions has become a focus for flavoenzyme chemistry in recent years[157-159]. With the exception of long-range electron transfer [160] and flavinylation[161], the N5 position is the point of entry for electrons from substrate molecules to form the reduced flavin. The role of the reduced flavin as a nucleophile in the formation of adducts at N5 is well-supported[162-164]. However, many of the recently discovered enzymes purported to utilize the N5 position of the isoalloxazine have proposed chemical mechanisms, for which key details remain unsettled[126, 130, 141]; this is particularly true for oxygenase chemistry. Nonetheless, in the reduced state of the flavin broad reactivity propensities can be identified for the C4a and N5 positions. The flavin-C4a position is more often involved in one-electron chemistry; commonly the reductive activation of molecular oxygen and formation of C4a-peroxo adducts or hydrogen peroxide[165]. Conversely, the N5 position is more often the site for two-electron reactivity forming covalent intermediates. However, the intermediacy of semiquinone forms that have high spin density at the C4a (blue semiquinone) or N5 (red semiquinone) suggests that one-electron reactivity is possible at either center, and this remains a source for mechanistic conjecture[126, 152, 166]. Scheme 8 summarizes the proposed chemistries of

reduced flavins with respect to the C4a and N5 positions and includes hypothetical pathways for N5 oxygenation.

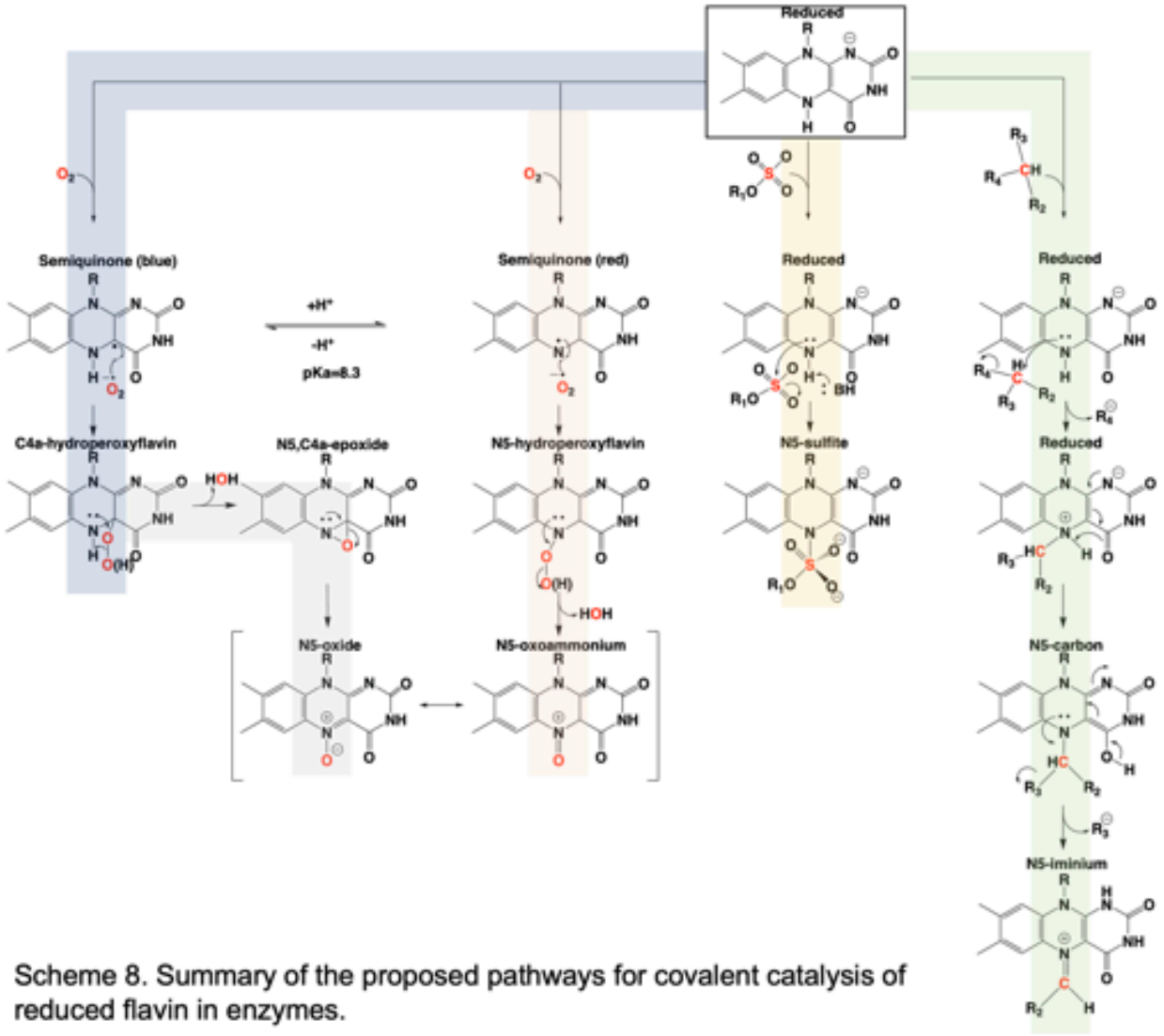

Scheme 8. Summary of the proposed pathways for covalent catalysis of reduced flavin in enzymes.

In conclusion, the adjacent C4a and N5 positions of the reduced isoalloxazine provide broad and tunable capabilities to flavin-dependent enzymes. The versatility of these centers is most evident in the fact that they cannot currently be definitively predicted from sequence and/or structure to perform a specific type of chemistry[125]. It would appear that C4a and N5 each

have dominant chemical propensities in enzymes but, each to some extent can be adapted to functions that are more commonly attributed the other.

[1] Sobrado, P. (2012) Noncanonical reactions of flavoenzymes, *Int J Mol Sci 13*, 14219-14242.
[2] Walker, W. H., Hemmerich, P., and Massey, V. (1967) [Reductive photoalkylation of flavin nuclei and flavin-catalyzed photodecarboxylation of phenylacetate], *Helv Chim Acta 50*, 2269-2279.
[3] Macheroux, P., Schmid, J., Amrhein, N., and Schaller, A. (1999) A unique reaction in a common pathway: mechanism and function of chorismate synthase in the shikimate pathway, *Planta 207*, 325-334.
[4] Massey, V., Muller, F., Feldberg, R., Schuman, M., Sullivan, P. A., Howell, L. G., Mayhew, S. G., Matthews, R. G., and Foust, G. P. (1969) The reactivity of flavoproteins with sulfite. Possible relevance to the problem of oxygen reactivity, *J Biol Chem 244*, 3999-4006.
[5] Muller, F., and Massey, V. (1969) Flavin-sulfite complexes and their structures, *J Biol Chem 244*, 4007-4016.
[6] Michaels, G. B., Davidson, J. T., and Peck, H. D., Jr. (1970) A flavin-sulfite adduct as an intermediate in the reaction catalyzed by adenylyl sulfate reductase from Desulfovibrio vulgaris, *Biochem Biophys Res Commun 39*, 321-328.
[7] Mattevi, A., Fraaije, M. W., Mozzarelli, A., Olivi, L., Coda, A., and van Berkel, W. J. (1997) Crystal structures and inhibitor binding in the octameric flavoenzyme vanillyl-alcohol oxidase: the shape of the active-site cavity controls substrate specificity, *Structure 5*, 907-920.
[8] Alston, T. A., Porter, D. J., and Bright, H. J. (1983) Suicide inactivation of D-amino acid oxidase by 1-chloro-1-nitroethane, *J Biol Chem 258*, 1136-1141.
[9] Porter, D. J., Voet, J. G., and Bright, H. J. (1973) Direct evidence for carbanions and covalent N 5 -flavin-carbanion adducts as catalytic intermediates in the oxidation of nitroethane by D-amino acid oxidase, *J Biol Chem 248*, 4400-4416.
[10] Ghisla, S., Ogata, H., Massey, V., Schonbrunn, A., Abeles, R. H., and Walsh, C. T. (1976) Kinetic studies on the inactivation of L-lactate oxidase by [the acetylenic suicide substrate] 2-hydroxy-3-butynoate, *Biochemistry 15*, 1791-1797.
[11] Silverman, R. B., Hiebert, C. K., and Vazquez, M. L. (1985) Inactivation of monoamine oxidase by allylamine does not result in flavin attachment, *J.Biol.Chem. 250*, 14648-14652.
[12] Mattevi, A., Vanoni, M. A., and Curti, B. (1997) Structure of D-amino acid oxidase: New insights from an old enzyme, *Current Opinion in Structural Biology 7*, 804-810.
[13] Fraaije, M. W., van den Heuvel, R. H., Roelofs, J. C., and van Berkel, W. J. (1998) Kinetic mechanism of vanillyl-alcohol oxidase with short-chain 4-alkylphenols, *Eur J Biochem 253*, 712-719.
[14] Binda, C., Angelini, R., Federico, R., Ascenzi, P., and Mattevi, A. (2001) Structural bases for inhibitor binding and catalysis in polyamine oxidase, *Biochemistry 40*, 2766-2776.
[15] Gadda, G., Edmondson, R. D., Russel, D. H., and Fitzpatrick, P. F. (1997) Identification of the naturally occurring flavin of nitroalkane oxidase from Fusarium oxysporum as a 5-nitrobutyl-FAD and conversion of the enzyme to the active FAD-containing form, *J.Biol.Chem. 272*.
[16] Fritz, G., Roth, A., Schiffer, A., Buchert, T., Bourenkov, G., Bartunik, H. D., Huber, H., Stetter, K. O., Kroneck, P. M., and Ermler, U. (2002) Structure of adenylylsulfate reductase from

the hyperthermophilic Archaeoglobus fulgidus at 1.6-A resolution, *Proc Natl Acad Sci U S A 99*, 1836-1841.
[17] Howlett, B. J., and Bar-Tana, J. (1980) Polyprenyl p-hydroxybenzoate carboxylase in flagellation of Salmonella typhimurium, *Journal of bacteriology 143*, 644-651.
[18] Leppik, R. A., Young, I. G., and Gibson, F. (1976) Membrane-associated reactions in ubiquinone biosynthesis in Escherichia coli. 3-Octaprenyl-4-hydroxybenzoate carboxy-lyase, *Biochimica et Biophysica Acta 436*, 800-810.
[19] Cox, G. B., Young, I. G., McCann, L. M., and Gibson, F. (1969) Biosynthesis of ubiquinone in Escherichia coli K-12: location of genes affecting the metabolism of 3-octaprenyl-4-hydroxybenzoic acid and 2-octaprenylphenol, *Journal of bacteriology 99*, 450-458.
[20] Meganathan, R. (2001) Ubiquinone biosynthesis in microorganisms, *Fems Microbiol Lett 203*, 131-139.
[21] Aussel, L., Pierrel, F., Loiseau, L., Lombard, M., Fontecave, M., and Barras, F. (2014) Biosynthesis and physiology of coenzyme Q in bacteria, *Biochimica et Biophysica Acta 1837*, 1004-1011.
[22] Gulmezian, M., Hyman, K. R., Marbois, B. N., Clarke, C. F., and Javor, G. T. (2007) The role of UbiX in Escherichia coli coenzyme Q biosynthesis, *Archives of biochemistry and biophysics 467*, 144-153.
[23] Zhang, H., and Javor, G. T. (2000) Identification of the ubiD gene on the Escherichia coli chromosome, *Journal of bacteriology 182*, 6243-6246.
[24] Stratford, M., Plumridge, A., and Archer, D. B. (2007) Decarboxylation of sorbic acid by spoilage yeasts is associated with the PAD1 gene, *Applied and environmental microbiology 73*, 6534-6542.
[25] Mukai, N., Masaki, K., Fujii, T., Kawamukai, M., and Iefuji, H. (2010) PAD1 and FDC1 are essential for the decarboxylation of phenylacrylic acids in Saccharomyces cerevisiae, *J Biosci Bioeng 109*, 564-569.
[26] Richard, P., Viljanen, K., and Penttila, M. (2015) Overexpression of PAD1 and FDC1 results in significant cinnamic acid decarboxylase activity in Saccharomyces cerevisiae, *AMB Express 5*, 12.
[27] Clausen, M., Lamb, C. J., Megnet, R., and Doerner, P. W. (1994) PAD1 encodes phenylacrylic acid decarboxylase which confers resistance to cinnamic acid in Saccharomyces cerevisiae, *Gene 142*, 107-112.
[28] Zhang, H., and Javor, G. T. (2003) Regulation of the isofunctional genes ubiD and ubiX of the ubiquinone biosynthetic pathway of Escherichia coli, *Fems Microbiol Lett 223*, 67-72.
[29] Liu, J., and Liu, J. H. (2006) Ubiquinone (coenzyme Q) biosynthesis in Chlamydophila pneumoniae AR39: identification of the ubiD gene, *Acta Biochim Biophys Sin (Shanghai) 38*, 725-730.
[30] Jacewicz, A., Izumi, A., Brunner, K., Schnell, R., and Schneider, G. (2013) Structural insights into the UbiD protein family from the crystal structure of PA0254 from Pseudomonas aeruginosa, *PLoS One 8*, e63161.
[31] Do, H., Kim, S. J., Lee, C. W., Kim, H. W., Park, H. H., Kim, H. M., Park, H., and Lee, J. H. (2015) Crystal structure of UbiX, an aromatic acid decarboxylase from the psychrophilic bacterium Colwellia psychrerythraea that undergoes FMN-induced conformational changes, *Scientific reports 5*, 8196.

[32] Larsson, S., Nilvebrant, N. O., and Jonsson, L. J. (2001) Effect of overexpression of Saccharomyces cerevisiae Pad1p on the resistance to phenylacrylic acids and lignocellulose hydrolysates under aerobic and oxygen-limited conditions, *Applied microbiology and biotechnology 57*, 167-174.
[33] Lin, F., Ferguson, K. L., Boyer, D. R., Lin, X. N., and Marsh, E. N. (2015) Isofunctional enzymes PAD1 and UbiX catalyze formation of a novel cofactor required by ferulic acid decarboxylase and 4-hydroxy-3-polyprenylbenzoic acid decarboxylase, *ACS Chem Biol 10*, 1137-1144.
[34] White, M. D., Payne, K. A., Fisher, K., Marshall, S. A., Parker, D., Rattray, N. J., Trivedi, D. K., Goodacre, R., Rigby, S. E., Scrutton, N. S., Hay, S., and Leys, D. (2015) UbiX is a flavin prenyltransferase required for bacterial ubiquinone biosynthesis, *Nature 522*, 502-506.
[35] Payne, K. A., White, M. D., Fisher, K., Khara, B., Bailey, S. S., Parker, D., Rattray, N. J., Trivedi, D. K., Goodacre, R., Beveridge, R., Barran, P., Rigby, S. E., Scrutton, N. S., Hay, S., and Leys, D. (2015) New cofactor supports alpha,beta-unsaturated acid decarboxylation via 1,3-dipolar cycloaddition, *Nature 522*, 497-501.
[36] Majer, F., Schmid, D. G., Altena, K., Bierbaum, G., and Kupke, T. (2002) The flavoprotein MrsD catalyzes the oxidative decarboxylation reaction involved in formation of the peptidoglycan biosynthesis inhibitor mersacidin, *Journal of bacteriology 184*, 1234-1243.
[37] Blaesse, M., Kupke, T., Huber, R., and Steinbacher, S. (2000) Crystal structure of the peptidyl-cysteine decarboxylase EpiD complexed with a pentapeptide substrate, *The EMBO journal 19*, 6299-6310.
[38] Blaesse, M., Kupke, T., Huber, R., and Steinbacher, S. (2003) Structure of MrsD, an FAD-binding protein of the HFCD family, *Acta crystallographica. Section D, Biological crystallography 59*, 1414-1421.
[39] Kopec, J., Schnell, R., and Schneider, G. (2011) Structure of PA4019, a putative aromatic acid decarboxylase from Pseudomonas aeruginosa, *Acta crystallographica. Section F, Structural biology and crystallization communications 67*, 1184-1188.
[40] Steinbacher, S., Hernandez-Acosta, P., Bieseler, B., Blaesse, M., Huber, R., Culianez-Macia, F. A., and Kupke, T. (2003) Crystal structure of the plant PPC decarboxylase AtHAL3a complexed with an ene-thiol reaction intermediate, *Journal of molecular biology 327*, 193-202.
[41] Kupke, T., Hernandez-Acosta, P., Steinbacher, S., and Culianez-Macia, F. A. (2001) Arabidopsis thaliana flavoprotein AtHAL3a catalyzes the decarboxylation of 4'-Phosphopantothenoylcysteine to 4'-phosphopantetheine, a key step in coenzyme A biosynthesis, *The Journal of biological chemistry 276*, 19190-19196.
[42] Manoj, N., and Ealick, S. E. (2003) Unusual space-group pseudosymmetry in crystals of human phosphopantothenoylcysteine decarboxylase, *Acta crystallographica. Section D, Biological crystallography 59*, 1762-1766.
[43] Gao, Y., Honzatko, R. B., and Peters, R. J. (2012) Terpenoid synthase structures: a so far incomplete view of complex catalysis, *Natural product reports 29*, 1153-1175.
[44] Doud, E. H., Perlstein, D. L., Wolpert, M., Cane, D. E., and Walker, S. (2011) Two distinct mechanisms for TIM barrel prenyltransferases in bacteria, *Journal of the American Chemical Society 133*, 1270-1273.

[45] Lupoli, T. J., Tsukamoto, H., Doud, E. H., Wang, T. S., Walker, S., and Kahne, D. (2011) Transpeptidase-mediated incorporation of D-amino acids into bacterial peptidoglycan, *Journal of the American Chemical Society 133*, 10748-10751.
[46] Bailey, S. S., Payne, K. A. P., Fisher, K., Marshall, S. A., Cliff, M. J., Spiess, R., Parker, D. A., Rigby, S. E. J., and Leys, D. (2018) The role of conserved residues in Fdc decarboxylase in prenylated flavin mononucleotide oxidative maturation, cofactor isomerization, and catalysis, *J Biol Chem 293*, 2272-2287.
[47] Christendat, D., Yee, A., Dharamsi, A., Kluger, Y., Savchenko, A., Cort, J. R., Booth, V., Mackereth, C. D., Saridakis, V., Ekiel, I., Kozlov, G., Maxwell, K. L., Wu, N., McIntosh, L. P., Gehring, K., Kennedy, M. A., Davidson, A. R., Pai, E. F., Gerstein, M., Edwards, A. M., and Arrowsmith, C. H. (2000) Structural proteomics of an archaeon, *Nature structural biology 7*, 903-909.
[48] Walsh, C. T., and Wencewicz, T. A. (2013) Flavoenzymes: versatile catalysts in biosynthetic pathways, *Natural product reports 30*, 175-200.
[49] Koehn, E. M., and Kohen, A. (2010) Flavin-dependent thymidylate synthase: a novel pathway towards thymine, *Archives of biochemistry and biophysics 493*, 96-102.
[50] Huisgen, R. (1963) 1,3-Dipolar Cycloadditions. Past and Future, *Angew. Chem. Int. Ed. Engl 2*.
[51] Prantz, K., and Mulzer, J. (2010) Synthetic applications of the carbonyl generating Grob fragmentation, *Chemical Reviews 110*, 3741-3766.
[52] Adak, S., and Begley, T. P. (2019) Hexachlorobenzene Catabolism Involves a Nucleophilic Aromatic Substitution and Flavin-N5-Oxide Formation, *Biochemistry 58*, 1181-1183.
[53] Bailey, S. S., Payne, K. A. P., Saaret, A., Marshall, S. A., Gostimskaya, I., Kosov, I., Fisher, K., Hay, S., and Leys, D. (2019) Enzymatic control of cycloadduct conformation ensures reversible 1,3-dipolar cycloaddition in a prFMN-dependent decarboxylase, *Nat Chem 11*, 1049-1057.
[54] Ferguson, K. L., Arunrattanamook, N., and Marsh, E. N. (2016) Mechanism of the Novel Prenylated Flavin-Containing Enzyme Ferulic Acid Decarboxylase Probed by Isotope Effects and Linear Free-Energy Relationships, *Biochemistry 55*, 2857-2863.
[55] Ferguson, K. L., Eschweiler, J. D., Ruotolo, B. T., and Marsh, E. N. G. (2017) Evidence for a 1,3-Dipolar Cyclo-addition Mechanism in the Decarboxylation of Phenylacrylic Acids Catalyzed by Ferulic Acid Decarboxylase, *J Am Chem Soc 139*, 10972-10975.
[56] Nassau, P. M., Martin, S. L., Brown, R. E., Weston, A., Monsey, D., McNeil, M. R., and Duncan, K. (1996) Galactofuranose biosynthesis in Escherichia coli K-12: identification and cloning of UDP-galactopyranose mutase, *Journal of bacteriology 178*, 1047-1052.
[57] Beverley, S. M., Owens, K. L., Showalter, M., Griffith, C. L., Doering, T. L., Jones, V. C., and McNeil, M. R. (2005) Eukaryotic UDP-galactopyranose mutase (GLF gene) in microbial and metazoal pathogens, *Eukaryotic cell 4*, 1147-1154.
[58] Koplin, R., Brisson, J. R., and Whitfield, C. (1997) UDP-galactofuranose precursor required for formation of the lipopolysaccharide O antigen of Klebsiella pneumoniae serotype O1 is synthesized by the product of the rfbDKPO1 gene, *The Journal of biological chemistry 272*, 4121-4128.

[59] Weston, A., Stern, R. J., Lee, R. E., Nassau, P. M., Monsey, D., Martin, S. L., Scherman, M. S., Besra, G. S., Duncan, K., and McNeil, M. R. (1997) Biosynthetic origin of mycobacterial cell wall galactofuranosyl residues, *Tuber Lung Dis 78*, 123-131.
[60] Novelli, J. F., Chaudhary, K., Canovas, J., Benner, J. S., Madinger, C. L., Kelly, P., Hodgkin, J., and Carlow, C. K. (2009) Characterization of the Caenorhabditis elegans UDP-galactopyranose mutase homolog glf-1 reveals an essential role for galactofuranose metabolism in nematode surface coat synthesis, *Dev Biol 335*, 340-355.
[61] Pan, F., Jackson, M., Ma, Y., and McNeil, M. (2001) Cell wall core galactofuran synthesis is essential for growth of mycobacteria, *Journal of bacteriology 183*, 3991-3998.
[62] Latge, J. P. (1999) Aspergillus fumigatus and aspergillosis, *Clin Microbiol Rev 12*, 310-350.
[63] Schmalhorst, P. S., Krappmann, S., Vervecken, W., Rohde, M., Muller, M., Braus, G. H., Contreras, R., Braun, A., Bakker, H., and Routier, F. H. (2008) Contribution of galactofuranose to the virulence of the opportunistic pathogen Aspergillus fumigatus, *Eukaryotic cell 7*, 1268-1277.
[64] Turco, S. J., and Descoteaux, A. (1992) The lipophosphoglycan of Leishmania parasites, *Annual review of microbiology 46*, 65-94.
[65] Kleczka, B., Lamerz, A. C., van Zandbergen, G., Wenzel, A., Gerardy-Schahn, R., Wiese, M., and Routier, F. H. (2007) Targeted gene deletion of Leishmania major UDP-galactopyranose mutase leads to attenuated virulence, *The Journal of biological chemistry 282*, 10498-10505.
[66] Richards, M. R., and Lowary, T. L. (2009) Chemistry and biology of galactofuranose-containing polysaccharides, *Chembiochem : a European journal of chemical biology 10*, 1920-1938.
[67] Partha, S. K., Sadeghi-Khomami, A., Slowski, K., Kotake, T., Thomas, N. R., Jakeman, D. L., and Sanders, D. A. (2010) Chemoenzymatic synthesis, inhibition studies, and X-ray crystallographic analysis of the phosphono analog of UDP-Galp as an inhibitor and mechanistic probe for UDP-galactopyranose mutase, *Journal of molecular biology 403*, 578-590.
[68] Veerapen, N., Yuan, Y., Sanders, D. A., and Pinto, B. M. (2004) Synthesis of novel ammonium and selenonium ions and their evaluation as inhibitors of UDP-galactopyranose mutase, *Carbohydr Res 339*, 2205-2217.
[69] Itoh, K., S., H. Z., and Liu, H. W. (2007) *Organic letters 9*, 3.
[70] Kuppala, R., Borrelli, S., Slowski, K., Sanders, D. A., Ravindranathan Kartha, K. P., and Pinto, B. M. (2015) Synthesis and biological evaluation of nonionic substrate mimics of UDP-Galp as candidate inhibitors of UDP galactopyranose mutase (UGM), *Bioorganic & medicinal chemistry letters 25*, 1995-1997.
[71] El Bkassiny, S., N'Go, I., Sevrain, C. M., Tikad, A., and Vincent, S. P. (2014) Synthesis of a novel UDP-carbasugar as UDP-galactopyranose mutase inhibitor, *Organic letters 16*, 2462-2465.
[72] Mahdavi-Amiri, Y., Mohan, S., Borrelli, S., Slowski, K., Sanders, D. A., and Pinto, B. M. (2016) Mechanism-based candidate inhibitors of uridine diphosphate galactopyranose mutase (UGM), *Carbohydr Res 419*, 1-7.

[73] Borrelli, S., Zandberg, W. F., Mohan, S., Ko, M., Martinez-Gutierrez, F., Partha, S. K., Sanders, D. A., Av-Gay, Y., and Pinto, B. M. (2010) Antimycobacterial activity of UDP-galactopyranose mutase inhibitors, *Int J Antimicrob Agents 36*, 364-368.
[74] Dykhuizen, E. C., May, J. F., Tongpenyai, A., and Kiessling, L. L. (2008) Inhibitors of UDP-galactopyranose mutase thwart mycobacterial growth, *Journal of the American Chemical Society 130*, 6706-6707.
[75] Soltero-Higgin, M., Carlson, E. E., Phillips, J. H., and Kiessling, L. L. (2004) Identification of inhibitors for UDP-galactopyranose mutase, *Journal of the American Chemical Society 126*, 10532-10533.
[76] Kashif, M., Tabrez, S., Husein, A., Arish, M., Kalaiarasan, P., Manna, P. P., Subbarao, N., Akhter, Y., and Rub, A. (2018) Identification of novel inhibitors against UDP-galactopyranose mutase to combat leishmaniasis, *J Cell Biochem 119*, 2653-2665.
[77] Zhang, Q., and Liu, H. (2001) Mechanistic investigation of UDP-galactopyranose mutase from Escherichia coli using 2- and 3-fluorinated UDP-galactofuranose as probes, *Journal of the American Chemical Society 123*, 6756-6766.
[78] Oppenheimer, M., Poulin, M. B., Lowary, T. L., Helm, R. F., and Sobrado, P. (2010) Characterization of recombinant UDP-galactopyranose mutase from Aspergillus fumigatus, *Archives of biochemistry and biophysics 502*, 31-38.
[79] Goni, G., Serrano, A., Frago, S., Hervas, M., Peregrina, J. R., De la Rosa, M. A., Gomez-Moreno, C., Navarro, J. A., and Medina, M. (2008) Flavodoxin-mediated electron transfer from photosystem I to ferredoxin-NADP+ reductase in Anabaena: role of flavodoxin hydrophobic residues in protein-protein interactions, *Biochemistry 47*, 1207-1217.
[80] Sanders, D. A., Staines, A. G., McMahon, S. A., McNeil, M. R., Whitfield, C., and Naismith, J. H. (2001) UDP-galactopyranose mutase has a novel structure and mechanism, *Nature structural biology 8*, 858-863.
[81] Oppenheimer, M., Valenciano, A. L., and Sobrado, P. (2011) Isolation and characterization of functional Leishmania major virulence factor UDP-galactopyranose mutase, *Biochemical and biophysical research communications 407*, 552-556.
[82] Zhang, Q., and Liu, H. W. (2000) Studies of UDP-Galactopyranose Mutase from Escherichia coli: An Unusual Role of Reduced FAD in Its Catalysis, *Journal of the American Chemical Society 122*, 5.
[83] Maaliki, C., Fu, J., Villaume, S., Viljoen, A., Raynaud, C., Hammoud, S., Thibonnet, J., Kremer, L., Vincent, S. P., and Thiery, E. (2020) Synthesis and evaluation of heterocycle structures as potential inhibitors of Mycobacterium tuberculosis UGM, *Bioorg Med Chem 28*, 115579.
[84] Oppenheimer, M., Valenciano, A. L., Kizjakina, K., Qi, J., and Sobrado, P. (2012) Chemical mechanism of UDP-galactopyranose mutase from Trypanosoma cruzi: a potential drug target against Chagas' disease, *PLoS One 7*, e32918.
[85] Dhatwalia, R., Singh, H., Solano, L. M., Oppenheimer, M., Robinson, R. M., Ellerbrock, J. F., Sobrado, P., and Tanner, J. J. (2012) Identification of the NAD(P)H binding site of eukaryotic UDP-galactopyranose mutase, *Journal of the American Chemical Society 134*, 18132-18138.

[86] Fonseca, I. O., Kizjakina, K., and Sobrado, P. (2013) UDP-galactopyranose mutases from Leishmania species that cause visceral and cutaneous leishmaniasis, *Archives of biochemistry and biophysics 538*, 103-110.
[87] Tanner, J. J., Boechi, L., Andrew McCammon, J., and Sobrado, P. (2014) Structure, mechanism, and dynamics of UDP-galactopyranose mutase, *Archives of biochemistry and biophysics 544*, 128-141.
[88] Barlow, J. N., Girvin, M. E., and Blanchard, J. S. (1999) Positional Isope Exchange Catalyzed by UDP-galactopyranose Mutase, *Journal of the American Chemical Society 121*, 11.
[89] Gusarov, I., Starodubtseva, M., Wang, Z. Q., McQuade, L., Lippard, S. J., Stuehr, D. J., and Nudler, E. (2008) Bacterial nitric-oxide synthases operate without a dedicated redox partner, *The Journal of biological chemistry 283*, 13140-13147.
[90] van Straaten, K. E., Routier, F. H., and Sanders, D. A. (2012) Structural insight into the unique substrate binding mechanism and flavin redox state of UDP-galactopyranose mutase from Aspergillus fumigatus, *The Journal of biological chemistry 287*, 10780-10790.
[91] van Straaten, K. E., Routier, F. H., and Sanders, D. A. (2012) Towards the crystal structure elucidation of eukaryotic UDP-galactopyranose mutase, *Acta crystallographica. Section F, Structural biology and crystallization communications 68*, 455-459.
[92] van Straaten, K. E., Kuttiyatveetil, J. R., Sevrain, C. M., Villaume, S. A., Jimenez-Barbero, J., Linclau, B., Vincent, S. P., and Sanders, D. A. (2015) Structural basis of ligand binding to UDP-galactopyranose mutase from Mycobacterium tuberculosis using substrate and tetrafluorinated substrate analogues, *Journal of the American Chemical Society 137*, 1230-1244.
[93] Gruber, T. D., Westler, W. M., Kiessling, L. L., and Forest, K. T. (2009) X-ray crystallography reveals a reduced substrate complex of UDP-galactopyranose mutase poised for covalent catalysis by flavin, *Biochemistry 48*, 9171-9173.
[94] Partha, S. K., van Straaten, K. E., and Sanders, D. A. (2009) Structural basis of substrate binding to UDP-galactopyranose mutase: crystal structures in the reduced and oxidized state complexed with UDP-galactopyranose and UDP, *Journal of molecular biology 394*, 864-877.
[95] Sun, H. G., Ruszczycky, M. W., Chang, W. C., Thibodeaux, C. J., and Liu, H. W. (2012) Nucleophilic participation of reduced flavin coenzyme in mechanism of UDP-galactopyranose mutase, *The Journal of biological chemistry 287*, 4602-4608.
[96] Huang, Z., Zhang, Q., and Liu, H. W. (2003) Reconstitution of UDP-galactopyranose mutase with 1-deaza-FAD and 5-deaza-FAD: analysis and mechanistic implications, *Bioorg Chem 31*, 494-502.
[97] Soltero-Higgin, M., Carlson, E. E., Gruber, T. D., and Kiessling, L. L. (2004) A unique catalytic mechanism for UDP-galactopyranose mutase, *Nat Struct Mol Biol 11*, 539-543.
[98] Mehra-Chaudhary, R., Dai, Y., Sobrado, P., and Tanner, J. J. (2016) In Crystallo Capture of a Covalent Intermediate in the UDP-Galactopyranose Mutase Reaction, *Biochemistry 55*, 833-836.
[99] Gruber, T. D., Borrok, M. J., Westler, W. M., Forest, K. T., and Kiessling, L. L. (2009) Ligand binding and substrate discrimination by UDP-galactopyranose mutase, *Journal of molecular biology 391*, 327-340.

[100] Soltero-Higgin, M., Carlson, E. E., Gruber, T. D., and Kiessling, L. L. (2004) A unique catalytic mechanism for UDP-galactopyranose mutase, *Nature structural & molecular biology 11*, 539-543.
[101] Pierdominici-Sottile, G., Cossio-Perez, R., Da Fonseca, I., Kizjakina, K., Tanner, J. J., and Sobrado, P. (2018) Steric Control of the Rate-Limiting Step of UDP-Galactopyranose Mutase, *Biochemistry 57*, 3713-3721.
[102] Dhatwalia, R., Singh, H., Oppenheimer, M., Sobrado, P., and Tanner, J. J. (2012) Crystal structures of Trypanosoma cruzi UDP-galactopyranose mutase implicate flexibility of the histidine loop in enzyme activation, *Biochemistry 51*, 4968-4979.
[103] Fullerton, S. W., Daff, S., Sanders, D. A., Ingledew, W. J., Whitfield, C., Chapman, S. K., and Naismith, J. H. (2003) Potentiometric analysis of UDP-galactopyranose mutase: stabilization of the flavosemiquinone by substrate, *Biochemistry 42*, 2104-2109.
[104] Huang, W., and Gauld, J. W. (2012) Tautomerization in the UDP-galactopyranose mutase mechanism: a DFT-cluster and QM/MM investigation, *The journal of physical chemistry. B 116*, 14040-14050.
[105] Cristescu, M. E., and Egbosimba, E. E. (2009) Evolutionary history of D-lactate dehydrogenases: a phylogenomic perspective on functional diversity in the FAD binding oxidoreductase/transferase type 4 family, *J Mol Evol 69*, 276-287.
[106] Beis, K., Srikannathasan, V., Liu, H., Fullerton, S. W., Bamford, V. A., Sanders, D. A., Whitfield, C., McNeil, M. R., and Naismith, J. H. (2005) Crystal structures of Mycobacteria tuberculosis and Klebsiella pneumoniae UDP-galactopyranose mutase in the oxidised state and Klebsiella pneumoniae UDP-galactopyranose mutase in the (active) reduced state, *Journal of molecular biology 348*, 971-982.
[107] Krissinel, E., and Henrick, K. (2004) Secondary-structure matching (SSM), a new tool for fast protein structure alignment in three dimensions, *Acta crystallographica. Section D, Biological crystallography 60*, 2256-2268.
[108] Poulin, M. B., Shi, Y., Protsko, C., Dalrymple, S. A., Sanders, D. A., Pinto, B. M., and Lowary, T. L. (2014) Specificity of a UDP-GalNAc pyranose-furanose mutase: a potential therapeutic target for Campylobacter jejuni infections, *Chembiochem : a European journal of chemical biology 15*, 47-56.
[109] Dhatwalia, R., Singh, H., Oppenheimer, M., Karr, D. B., Nix, J. C., Sobrado, P., and Tanner, J. J. (2012) Crystal structures and small-angle x-ray scattering analysis of UDP-galactopyranose mutase from the pathogenic fungus Aspergillus fumigatus, *The Journal of biological chemistry 287*, 9041-9051.
[110] Kincaid, V. A., London, N., Wangkanont, K., Wesener, D. A., Marcus, S. A., Heroux, A., Nedyalkova, L., Talaat, A. M., Forest, K. T., Shoichet, B. K., and Kiessling, L. L. (2015) Virtual Screening for UDP-Galactopyranose Mutase Ligands Identifies a New Class of Antimycobacterial Agents, *ACS Chem Biol 10*, 2209-2218.
[111] Da Fonseca, I., Qureshi, I. A., Mehra-Chaudhary, R., Kizjakina, K., Tanner, J. J., and Sobrado, P. (2014) Contributions of unique active site residues of eukaryotic UDP-galactopyranose mutases to substrate recognition and active site dynamics, *Biochemistry 53*, 7794-7804.
[112] Penman, G. A., Lockhart, D. E., Ferenbach, A., and van Aalten, D. M. (2012) Purification, crystallization and preliminary X-ray diffraction data of UDP-galactopyranose mutase

from Aspergillus fumigatus, *Acta crystallographica. Section F, Structural biology and crystallization communications 68*, 705-708.
[113] Derewenda, Z. S. (2004) Rational protein crystallization by mutational surface engineering, *Structure (Camb) 12*, 529-535.
[114] Goldschmidt, L., Cooper, D. R., Derewenda, Z. S., and Eisenberg, D. (2007) Toward rational protein crystallization: A Web server for the design of crystallizable protein variants, *Protein science : a publication of the Protein Society 16*, 1569-1576.
[115] Bottoms, C. A., Smith, P. E., and Tanner, J. J. (2002) A structurally conserved water molecule in Rossmann dinucleotide-binding domains, *Protein science : a publication of the Protein Society 11*, 2125-2137.
[116] Kleiger, G., and Eisenberg, D. (2002) GXXXG and GXXXA motifs stabilize FAD and NAD(P)-binding Rossmann folds through C(alpha)-H... O hydrogen bonds and van der waals interactions, *Journal of molecular biology 323*, 69-76.
[117] Wencewicz, T. A., and Walsh, C. T. (2012) Pseudomonas syringae self-protection from tabtoxinine-beta-lactam by ligase TblF and acetylase Ttr, *Biochemistry 51*, 7712-7725.
[118] Chaiyen, P., Fraaije, M. W., and Mattevi, A. (2012) The enigmatic reaction of flavins with oxygen, *Trends in biochemical sciences 37*, 373-380.
[119] Hemmerich, P., Nagelschneider, G., and Veeger, C. (1970) Chemistry and molecular biology of flavins and flavoproteins, *FEBS letters 8*, 69-83.
[120] Mansoorabadi, S. O., Thibodeaux, C. J., and Liu, H. W. (2007) The diverse roles of flavin coenzymes--nature's most versatile thespians, *The Journal of organic chemistry 72*, 6329-6342.
[121] Massey, V. (1994) Activation of molecular oxygen by flavins and flavoproteins, *The Journal of biological chemistry 269*, 22459-22462.
[122] Palfey, B. A., and McDonald, C. A. (2010) Control of catalysis in flavin-dependent monooxygenases, *Archives of biochemistry and biophysics 493*, 26-36.
[123] De Colibus, L., and Mattevi, A. (2006) New frontiers in structural flavoenzymology, *Curr Opin Struct Biol 16*, 722-728.
[124] Crozier-Reabe, K., and Moran, G. R. (2012) Form follows function: structural and catalytic variation in the class a flavoprotein monooxygenases, *Int J Mol Sci 13*, 15601-15639.
[125] Teufel, R., Miyanaga, A., Michaudel, Q., Stull, F., Louie, G., Noel, J. P., Baran, P. S., Palfey, B., and Moore, B. S. (2013) Flavin-mediated dual oxidation controls an enzymatic Favorskii-type rearrangement, *Nature 503*, 552-556.
[126] Teufel, R., Stull, F., Meehan, M. J., Michaudel, Q., Dorrestein, P. C., Palfey, B., and Moore, B. S. (2015) Biochemical Establishment and Characterization of EncM's Flavin-N5-oxide Cofactor, *Journal of the American Chemical Society 137*, 8078-8085.
[127] Piel, J., Hertweck, C., Shipley, P. R., Hunt, D. M., Newman, M. S., and Moore, B. S. (2000) Cloning, sequencing and analysis of the enterocin biosynthesis gene cluster from the marine isolate 'Streptomyces maritimus': evidence for the derailment of an aromatic polyketide synthase, *Chem Biol 7*, 943-955.
[128] Cheng, Q., Xiang, L., Izumikawa, M., Meluzzi, D., and Moore, B. S. (2007) Enzymatic total synthesis of enterocin polyketides, *Nature chemical biology 3*, 557-558.

[129] Hertweck, C., Xiang, L., Kalaitzis, J. A., Cheng, Q., Palzer, M., and Moore, B. S. (2004) Context-dependent behavior of the enterocin iterative polyketide synthase; a new model for ketoreduction, *Chem Biol 11*, 461-468.
[130] Xiang, L., Kalaitzis, J. A., and Moore, B. S. (2004) EncM, a versatile enterocin biosynthetic enzyme involved in Favorskii oxidative rearrangement, aldol condensation, and heterocycle-forming reactions, *P Natl Acad Sci USA 101*, 15609-15614.
[131] Seto, H., Sato, T., Urano, S., Uzawa, J., and Yonehara, H. (1976) Utilization of 13C-13C coupling in structural and biosynthetic studies. VII. The structure and biosynthesis of vulgamycin., *Tetrahedron Letters 48*, 3.
[132] Crosby, J., and Crump, M. P. (2012) The structural role of the carrier protein--active controller or passive carrier, *Natural product reports 29*, 1111-1137.
[133] Entsch, B., Ballou, D. P., and Massey, V. (1976) Role of oxygenated flavins in the catalytic reaction of p-hydroxybenzoate hydroxylase, In *Flavins and Flavoproteins* (18/0/15, B., Ed.), pp 111-123, Elsevier, Amsterdam.
[134] Entsch, B., and Ballou, D. P. (1989) Purification, properties, and oxygen reactivity of p-hydroxybenzoate hydroxylase from Pseudomonas aeruginosa, *Biochim Biophys Acta 999*, 313-322.
[135] Rastetter, W. H., Gadek, T. R., Tane, J. P., and Frost, J. W. (1979) Oxidations and oxygen transfers effected by a flavin N(5)-oxide. A model for flavin-dependent monooxygenases., *Journal of the American Chemical Society 101*, 3.
[136] Orf, H. W., and Dolphin, D. (1974) Oxaziridines as possible intermediates in flavin monooxygenases, *P Natl Acad Sci USA 71*, 2646-2650.
[137] Saleem-Batcha, R., Stull, F., Sanders, J. N., Moore, B. S., Palfey, B. A., Houk, K. N., and Teufel, R. (2018) Enzymatic control of dioxygen binding and functionalization of the flavin cofactor, *Proc Natl Acad Sci U S A 115*, 4909-4914.
[138] Massey, V. (1980) The biological and chemical versatility of riboflavin, *Univ.Mich.Med.Center J. 46*, 28-37.
[139] Barquera, B., Morgan, J. E., Lukoyanov, D., Scholes, C. P., Gennis, R. B., and Nilges, M. J. (2003) X- and W-band EPR and Q-band ENDOR studies of the flavin radical in the Na+ -translocating NADH:quinone oxidoreductase from Vibrio cholerae, *J Am Chem Soc 125*, 265-275.
[140] Adak, S., and Begley, T. P. (2016) Dibenzothiophene Catabolism Proceeds via a Flavin-N5-oxide Intermediate, *J Am Chem Soc 138*, 6424-6426.
[141] Adak, S., and Begley, T. P. (2017) RutA-Catalyzed Oxidative Cleavage of the Uracil Amide Involves Formation of a Flavin-N5-oxide, *Biochemistry 56*, 3708-3709.
[142] Mukherjee, T., Zhang, Y., Abdelwahed, S., Ealick, S. E., and Begley, T. P. (2010) Catalysis of a flavoenzyme-mediated amide hydrolysis, *J Am Chem Soc 132*, 5550-5551.
[143] Vogels, G. D., and Van der Drift, C. (1976) Degradation of purines and pyrimidines by microorganisms, *Bacteriol Rev 40*, 403-468.
[144] Wasternack, C. (1978) Degradation of Pyrimidines — Enzymes, Localization and Role in Metabolism, *Biochemie und Physiologie der Pflanzen 173*, 467-499.
[145] Rawls, J. M., Jr. (2006) Analysis of pyrimidine catabolism in Drosophila melanogaster using epistatic interactions with mutations of pyrimidine biosynthesis and beta-alanine metabolism, *Genetics 172*, 1665-1674.

[146] Piskur, J., Schnackerz, K. D., Andersen, G., and Bjornberg, O. (2007) Comparative genomics reveals novel biochemical pathways, *Trends Genet 23*, 369-372.
[147] Soong, C. L., Ogawa, J., and Shimizu, S. (2001) Novel amidohydrolytic reactions in oxidative pyrimidine metabolism: analysis of the barbiturase reaction and discovery of a novel enzyme, ureidomalonase, *Biochem Biophys Res Commun 286*, 222-226.
[148] Soong, C. L., Ogawa, J., Sakuradani, E., and Shimizu, S. (2002) Barbiturase, a novel zinc-containing amidohydrolase involved in oxidative pyrimidine metabolism, *J Biol Chem 277*, 7051-7058.
[149] Loh, K. D., Gyaneshwar, P., Markenscoff Papadimitriou, E., Fong, R., Kim, K. S., Parales, R., Zhou, Z., Inwood, W., and Kustu, S. (2006) A previously undescribed pathway for pyrimidine catabolism, *Proc Natl Acad Sci U S A 103*, 5114-5119.
[150] Ellis, H. R. (2010) The FMN-dependent two-component monooxygenase systems, *Archives of biochemistry and biophysics 497*, 1-12.
[151] Hall, A., Karplus, P. A., and Poole, L. B. (2009) Typical 2-Cys peroxiredoxins--structures, mechanisms and functions, *Febs J 276*, 2469-2477.
[152] Matthews, A., Saleem-Batcha, R., Sanders, J. N., Stull, F., Houk, K. N., and Teufel, R. (2020) Aminoperoxide adducts expand the catalytic repertoire of flavin monooxygenases, *Nature chemical biology 16*, 556-563.
[153] Mascotti, M. L., Juri Ayub, M., Furnham, N., Thornton, J. M., and Laskowski, R. A. (2016) Chopping and Changing: the Evolution of the Flavin-dependent Monooxygenases, *J Mol Biol 428*, 3131-3146.
[154] van Berkel, W. J., Kamerbeek, N. M., and Fraaije, M. W. (2006) Flavoprotein monooxygenases, a diverse class of oxidative biocatalysts, *Journal of biotechnology 124*, 670-689.
[155] McDonald, C. A., Fagan, R. L., Collard, F., Monnier, V. M., and Palfey, B. A. (2011) Oxygen reactivity in flavoenzymes: context matters, *J Am Chem Soc 133*, 16809-16811.
[156] Huijbers, M. M., Montersino, S., Westphal, A. H., Tischler, D., and van Berkel, W. J. (2014) Flavin dependent monooxygenases, *Arch Biochem Biophys 544*, 2-17.
[157] Piano, V., Palfey, B. A., and Mattevi, A. (2017) Flavins as Covalent Catalysts: New Mechanisms Emerge, *Trends in biochemical sciences 42*, 457-469.
[158] Leys, D., and Scrutton, N. S. (2020) Flavin doesn't put all oxygens in one basket, *Nature chemical biology 16*, 485-486.
[159] Romero, E., Gomez Castellanos, J. R., Gadda, G., Fraaije, M. W., and Mattevi, A. (2018) Same Substrate, Many Reactions: Oxygen Activation in Flavoenzymes, *Chem Rev 118*, 1742-1769.
[160] Schnackerz, K. D., Dobritzsch, D., Lindqvist, Y., and Cook, P. F. (2004) Dihydropyrimidine dehydrogenase: a flavoprotein with four iron-sulfur clusters, *Biochim Biophys Acta 1701*, 61-74.
[161] Sharma, P., Maklashina, E., Cecchini, G., and Iverson, T. M. (2018) Crystal structure of an assembly intermediate of respiratory Complex II, *Nat Commun 9*, 274.
[162] Sobrado, P., and Tanner, J. J. (2017) Multiple functionalities of reduced flavin in the non-redox reaction catalyzed by UDP-galactopyranose mutase, *Arch Biochem Biophys 632*, 59-65.

[163] Leys, D. (2018) Flavin metamorphosis: cofactor transformation through prenylation, *Curr Opin Chem Biol 47*, 117-125.
[164] Marshall, S. A., Payne, K. A. P., and Leys, D. (2017) The UbiX-UbiD system: The biosynthesis and use of prenylated flavin (prFMN), *Arch Biochem Biophys 632*, 209-221.
[165] Massey, V. (1994) Activation of molecular oxygen by flavins and flavoproteins, *J Biol Chem 269*, 22459-22462.
[166] Dai, Y., Valentino, H., and Sobrado, P. (2018) Evidence for the Formation of a Radical-Mediated Flavin-N5 Covalent Intermediate, *Chembiochem 19*, 1609-1612.